Tribology International 94 (2016) 509–529

Contents lists available at ScienceDirect

Tribology International

journal homepage: www.elsevier.com/locate/triboint

Hydrodynamic lubrication of textured surfaces: A review of modeling techniques and key findings

Daniel Gropper*, Ling Wang, Terry J. Harvey

National Centre for Advanced Tribology at Southampton (nCATS), Faculty of Engineering and the Environment, University of Southampton, Southampton SO17 1BJ, UK

ARTICLE INFO

Article history:
Received 22 August 2015
Received in revised form
1 October 2015
Accepted 7 October 2015
Available online 22 October 2015

Keywords:
Surface texture
Hydrodynamic lubrication
Numerical analysis
Cavitation

ABSTRACT

Understanding the influence of surface properties (roughness, grooves, discrete textures/dimples) on the performance of hydrodynamically lubricated contacts has been the aim of numerous studies. A variety of different numerical models have been employed by many researchers in order to find optimal texturing parameters (shape, size, distribution) for best performance enhancement in terms of load carrying capacity, film thickness, friction and wear. However, the large number of different modeling techniques and complexity in the patterns make finding the optimum texture a challenging task and have led to contrary conclusions. This article outlines the research effort on surface texturing worldwide, reviews the key findings and, in particular, provides a comparative summary of different modeling techniques for fluid flow, cavitation and micro-hydrodynamic effects.

© 2015 The Authors. Published by Elsevier Ltd. This is an open access article under the CC BY license (http://creativecommons.org/licenses/by/4.0/).

1. Introduction

Using textured surfaces for contact performance enhancement is not a new concept. For example, special surface structures can increase adhesion, enabling tree frogs to safely walk on wet surfaces [1] or reduce aerodynamic drag, making the movement of sharks in water more efficient [2]. The dimpled surface of a golf ball also highly reduces drag and allows it to fly up to four times as far when compared to a golf ball having a smooth surface [3].

Surface structures also have an influence on the tribological performance of lubricated contacts. In 1966, Hamilton et al. [4] found that micro irregularities on the surfaces of rotary-shaft seals were capable of producing hydrodynamic pressure and hence, created a load carrying capacity. They directly observed cavitation at the divergent part of asperities by using a transparent rotor and proposed that local cavitation was the responsible mechanism for the observed load support. Anno et al. [5,6] investigated this theory some years later and concluded that the introduction of micro-asperities was an efficient method for lubricating mechanical face seals and parallel rotating thrust bearings. One of the first successful commercial applications of surface texturing, however, was that of cylinder liners of combustion engines [7]. The micro-grooves on the liner surface produced by the honing process are able to retain oil and trap wear debris in the contact and thus increase lifetime. In the following three decades, rather little attention on textured surfaces was paid, with only a handful papers being published.

The research on surface texturing gained a new momentum in 1996, when Etsion's group published one of their first papers on surface texturing [8]. They used the incompressible, two-dimensional Reynolds equation together with the Half-Sommerfeld cavitation boundary condition to mathematically investigate mechanical seals with hemispherical dimples on one of the mating surfaces. They concluded that an increase in load carrying capacity was obtained due to local cavitation and that a proper selection of texture size and density was crucial. They conducted field tests to compare the performance of non-textured seals with textured ones and showed that texturing could increase seal lifetime threefold [9]. Since then, due to the promising results obtained by Etsion and co-workers, hundreds of theoretical and experimental studies have been conducted worldwide in order to improve the performance of tribological contacts (see Fig. 1(a)). A wide range of applications have been explored, including thrust bearings, journal bearings, cylinder liners, piston rings, concentrated contacts, mechanical seals, magnetic storage devices, piston pins and drill bits.

The vast majority of research in the field of surface texturing has been based on theoretical modeling (see Fig. 1(b)). Whereas early theoretical models were very limited, today's lubrication simulations are capable of including transient effects, mass-conserving and inter-asperity cavitation, temperature effects, deformation and asperity contact models.

Although promising results have been obtained, finding optimal texturing parameters is still very challenging due to the large

* Corresponding author.
E-mail address: D.Gropper@soton.ac.uk (D. Gropper).

http://dx.doi.org/10.1016/j.triboint.2015.10.009
0301-679X/© 2015 The Authors. Published by Elsevier Ltd. This is an open access article under the CC BY license (http://creativecommons.org/licenses/by/4.0/).

Nomenclature

a	dimension (m)
A_c	contact area (m^2)
A_{cell}	texture cell area (m^2)
$A_{texture}$	texture area (m^2)
$A_{textured}$	textured area (m^2)
b	dimension (m)
B	relative textured portion (dimensionless)
c	clearance (m)
e	eccentricity (m)
g	switch function (dimensionless)
h	local film thickness (m)
h_0	minimum film thickness (m)
h_1	inlet film thickness (m)
$h_{texture}$	maximum texture depth (m)
H_r	texture height ratio (dimensionless)
$K = h_1/h_0 - 1$	convergence ratio (dimensionless)
l	texture dimension in sliding direction (m)
N	total number of dimples (dimensionless)
p	local pressure (Pa)
p_{cav}	cavitation pressure (Pa)
p_{sup}	supply pressure (Pa)
Q	flow rate (m^3/s)
R_B	bearing radius (m)
R_i	inner radius (m)
R_J	journal radius (m)
R_o	outer radius (m)
Re	Reynolds number (dimensionless)
S	relative texture depth (dimensionless)
t	time (s)
$\boldsymbol{u}$	velocity vector (m/s)
u	velocity in x-direction (m/s)
v	velocity in y-direction (m/s)
w	velocity in z-direction (m/s)
x	Cartesian coordinate (m)
X_c	contact dimension in x-direction (m)
X_{cell}	cell dimension in x-direction (m)
$X_{textured}$	textured length in x-direction (m)
y	Cartesian coordinate (m)
Y_c	contact dimension in y-direction (m)
Y_{cell}	cell dimension in y-direction (m)
$Y_{textured}$	textured length in y-direction (m)
z	Cartesian coordinate (m)
α	relative texture extend in x- or φ-direction (dimensionless)
β	relative texture extend in y- or radial direction (dimensionless)
β	bulk modulus (Pa)
$\varepsilon = e/c$	relative eccentricity (dimensionless)
η	lubricant dynamic viscosity (Pa s)
θ	fractional film content (dimensionless)
λ	texture aspect ratio (dimensionless)
ρ	density (kg/m^3)
ρ_c	reference density (kg/m^3)
$\rho_{texture}$	texture density (dimensionless)
σ	surface rms roughness (m)
φ	angular coordinate (deg)
φ_c	contact dimension in φ-direction (deg)
$\varphi_{textured}$	textured portion in φ-direction (deg)
ϕ_x, ϕ_y	pressure flow factors (dimensionless)
ϕ_s	shear flow factor (dimensionless)
ω	rotational speed (1/s)

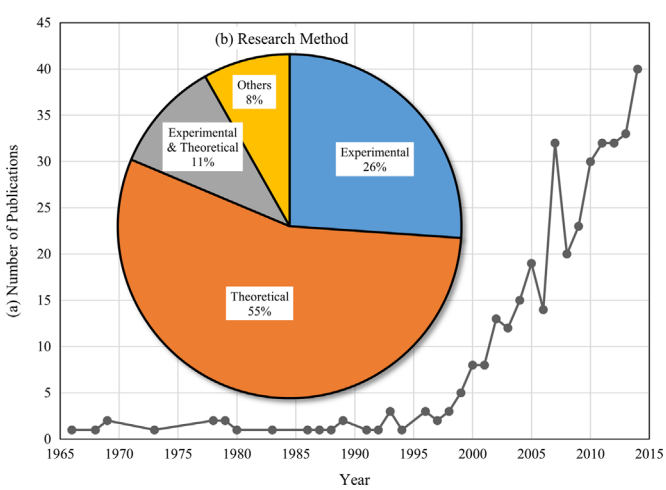

Fig. 1. Worldwide research effort on surface texturing over the last 50 years: (a) Number of publications per year and (b) Research method.

number of variables involved and the complexity of governing equations. Additionally, the optimal texture design seems to highly depend on the type of contact and operating conditions and in certain cases, textures have been reported to be detrimental, if designed wrong [10,11]. The aforementioned issues have led to contrary conclusions and make a successful industrial application of surface texturing still difficult. Another problem is the large variety of modeling techniques and lack of standard methods, which makes it very difficult to conduct numerical research, especially for new researchers in the field.

The purpose of this paper is to outline the research effort on surface texturing worldwide, review the key findings and, in particular, provide the reader with a comparative study of different modeling techniques and numerical methods commonly used to predict the performance of textured or rough surfaces. The current understandings on how texturing can improve the performance are discussed in the first part of this article, followed by a review on optimal texturing parameters proposed in literature for typical bearing applications. Methods and algorithms to describe fluid flow, cavitation phenomena and micro-hydrodynamic effects as well as different discretization methods and numerical procedures are reviewed and analysed in the second part of this paper.

A detailed review on the state of the art in surface texturing is a necessary first step in standardising mathematical models and restricting mistakes in this field. A consistent understanding of the phenomena involved and standard theoretical methods will improve and facilitate future research and the industrial application of this technology. This article is aimed at making a contribution in this direction.

2. Background

2.1. A survey of research on surface texturing

Hundreds of studies on the influence of rough/textured surfaces on tribological performance of lubricated contacts have been published since 1966. The vast majority has been published over the last two decades (see Fig. 1(a)). In an extensive literature

survey, the authors found close to 400 publications on rough and textured surfaces, published between 1966 and 2015.

Interestingly, more than 50% of the studies are purely theoretical, based on different forms of the Reynolds equation, Navier–Stokes equations or Stokes equations (see Fig. 1(b)). Models in the early years were based on the steady-state, two-dimensional Reynolds equation, applying non-mass-conserving cavitation boundary conditions and neglecting changes in viscosity, density and temperature. Also, surface deformations and the effect of surface roughness were not considered. Examples of more basic models can be found in [12–16] for journal bearings, in [8,17,18] for mechanical seals, in [19,20] for thrust bearings and in [21,22] for cylinder liners.

The development of more efficient algorithms and solution techniques combined with the increase in computational power available have led to much more sophisticated models, especially over the last 10 years. Papadopoulos et al. [23], for example, used commercial computational fluid dynamics (CFD) software to solve the Navier–Stokes and energy equations to study the effect of rectangular dimples on the performance of partially textured sector-pad thrust bearings. Kango et al. [24] investigated textured journal bearings using a generalized Reynolds equation. Their model is capable of describing viscous heat dissipation and non-Newtonian lubricant behavior and incorporates a mass-conserving cavitation algorithm based on the Jakobsson–Floberg–Olsson (JFO) boundary conditions. Han et al. [25] used a modified averaged Reynolds equation to study the effect of misalignment and shaft axial motion on the performance of journal bearings with rough surfaces under transient and mixed lubrication conditions.

Less than a third of all publications were based on experimental approaches only, of which the most commonly used are pin-on-disc [26–31] and ball-on-disc [32] setups as well as reciprocating sliding tests [33]. Some studies, however, were conducted on real components. Examples include journal bearings [34,35], thrust bearings [36–38] and seals [39–41].

About 11%, corresponding to 41 references in the authors' survey, describe both, experimental and theoretical investigations. The remaining 8% of publications analysed are, for example, reviews [9,42–47], publications on manufacturing techniques [48–50] and classification/characterization of textured surfaces [51]. Further results of the survey are given in respective sections.

A large number of researchers have contributed to today's knowledge around surface texturing, however, the still very limited number of successful industrial applications emphasizes the difficulties and challenges that are still encountered in this field. The following sections are thus intended to give the reader a brief overview of the key findings, common conclusions and some guidelines on texture design given in literature so far.

2.2. Definition of surface texturing

Surface texturing is the intentional introduction of well-defined identical features (discrete dimples, grooves) on surfaces. An example of a partially textured parallel thrust pad bearing can be seen in Fig. 2. In contrast to textures, surface roughness is generally considered random and not well characterized. However, some of the functions of textures described below can also be related to rough surfaces. For example, the valley between two adjacent asperities can be interpreted as a dimple.

2.3. Functions of surface textures

Surface textures may act as lubricant reservoirs [4,52], providing lubricant to the contact in cases of starved lubrication, and entrap wear debris [53,54], minimizing third-body abrasion. Although the aforementioned effects are often described in literature, consistent results do not exist and further research in this direction is needed. A textured surface also has an overall lower contact area, which can lead to a reduction of stiction [55]. The aforementioned mechanisms can reduce wear and thus increase durability. The most dominant effect, however, as well as the only one captured by theoretical models, is the creation of an additional hydrodynamic lift that can lead to a certain increase in load carrying capacity of the contact in cases of mixed and hydrodynamic lubrication. This can also lead to an expansion of the range of hydrodynamic lubrication [56]. Although this phenomenon of load support is not yet fully understood, some commonly accepted explanations exist.

One of the earliest explanations was the occurrence of local cavitation [4,9,17,57], which can lead to an asymmetric pressure distribution over a single texture, as negative pressures caused the divergent part of a texture are limited by the lubricant's cavitation pressure (see Fig. 3(a) and (b)). The occurrence of cavitation inside individual dimples was also shown experimentally by Qiu and Khonsari [38,58] and Zhang and Meng [59], using high speed cameras. Fig. 3(b) illustrates typical pressure distributions over a single, cell-centred texture for three different cases: (i) cavitation

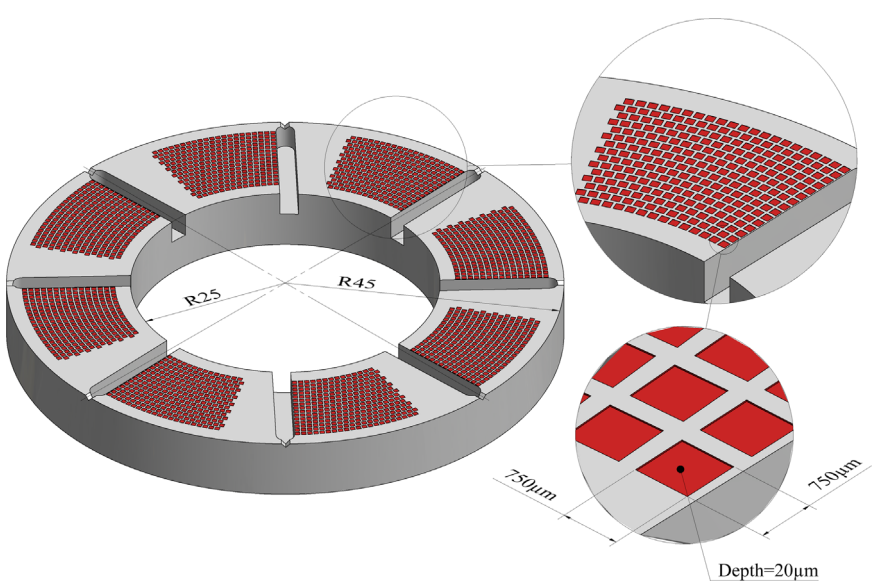

Fig. 2. Partially textured parallel thrust pad bearing with rectangular dimples (adapted from [193]).

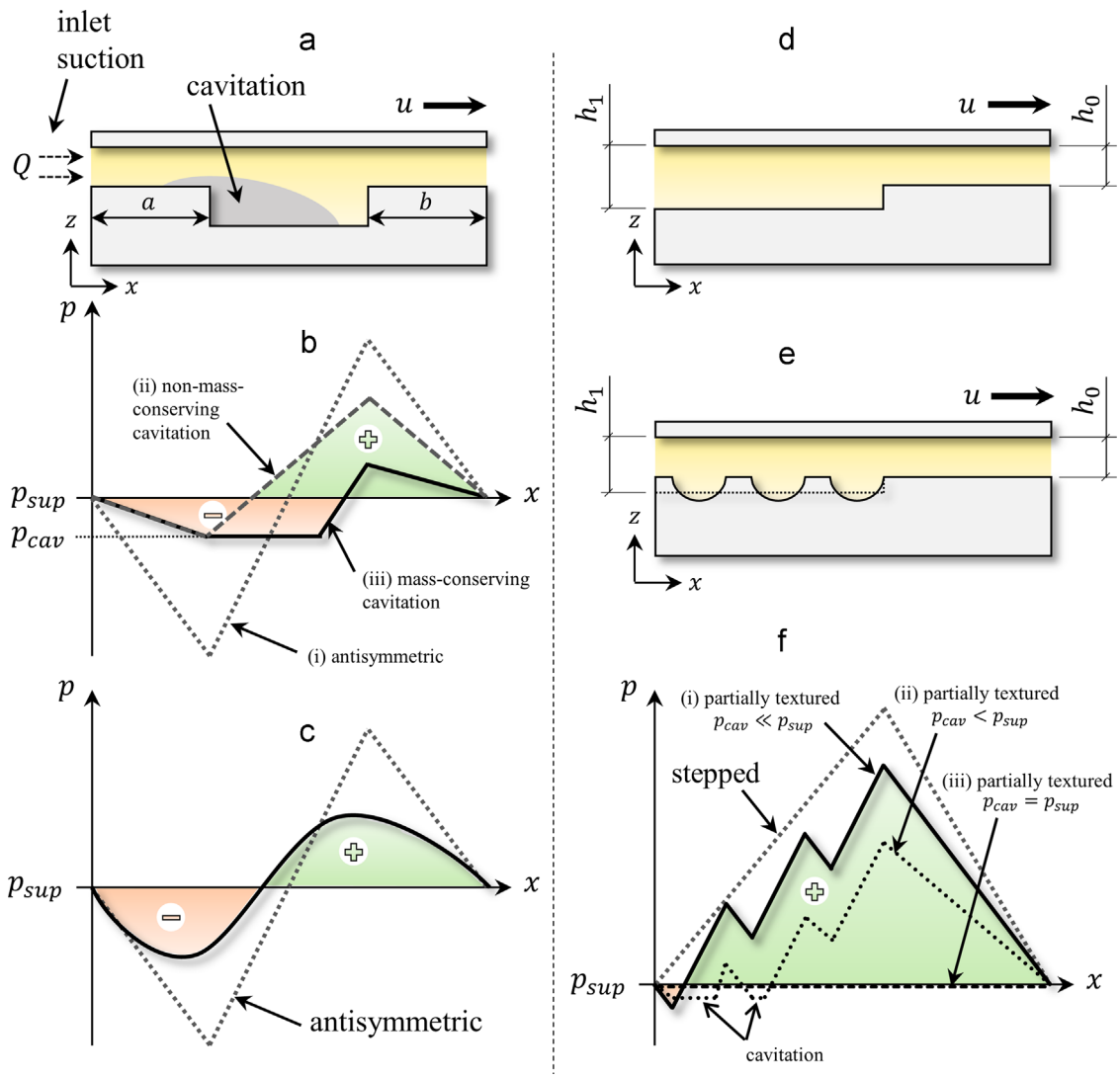

Fig. 3. (a) Single texture cell, (b) Typical pressure distribution over a single texture with cavitation, (c) Typical pressure distribution over a single texture with inertia effects, (d) Stepped slider, (e) Partially textured slider and (f) Typical pressure distributions over a stepped and partially textured slider.

does not occur ($p_{cav} \ll p_{sup}$), (ii) predicted by a non-mass-conserving cavitation algorithm for $p_{cav} < p_{sup}$ and (iii) predicted by a mass-conserving cavitation algorithm for $p_{cav} < p_{sup}$. Note, however, that load is only generated in certain cases, as the positive pressures are also influenced. In some cases the load support may even become negative, depending on the shape of the asymmetric pressure distribution. Additionally, lift can only be generated when the cavitation pressure is inferior to the supply pressure, as this will provide the necessary pressure gradient to ensure a sufficient lubricant supply (*inlet suction* [60,61], see Fig. 3(a)). If cavitation and supply pressure are equal this pressure gradient does not occur, leading to starvation in the dimple, hence, no pressure can build up. If the supply pressure is much higher than the cavitation pressure, cavitation will not occur at all. In this case the pressure distribution over a single texture is antisymmetric and no lift can be generated either.

The promising results concerning cell centred dimples published in early papers (e.g. [19]) were caused by the implementation of non-mass-conserving cavitation boundary conditions. The pressure distribution over a single cell-centred dimple obtained with a non-mass-conserving cavitation algorithm falsely predicts a high load support as compared to the solution of the same problem with a mass-conserving treatment of cavitation, as first discussed by Ausas et al. [62] in 2007 (see Fig. 3(b)).

Another way to obtain load carrying capacity is to shift the texture towards the inlet, i.e. $a < b$ in Fig. 3(a). This will always (even if cavitation does not occur at all) lead to a load carrying capacity as long as $p_{cav} < p_{sup}$. However, this configuration should be interpreted as *partial texturing*, where lift is generated in a more traditional geometrical way, as discussed below.

Ultimately, today's understanding is that, despite the fact that local cavitation effects obviously have a significant influence on the pressure distribution and thus load capacity, they can only in certain cases lead to additional load support in individual, cell-centred textures, i.e. fully textured contacts. The crucial factor here is the p_{cav}/p_{sup} ratio.

Tønder [63,64] suggested that the introduction of roughness at the inlet of a parallel sliding bearing provides a step-like configuration similar to a Rayleigh step bearing. It was also found that more lubricant is available in the pressure build-up zone as the roughness at the inlet could prevent leakage.

Another explanation for a *disturbed* pressure distribution over a single texture and thus in certain cases load carrying capacity are inertia-related effects (see Fig. 3(c)), which were first studied by Arghir et al. [65]. As simplified models based on the Reynolds equation or Stokes equations do not consider inertia effects, they solved the full Navier–Stokes equations for different macro-roughness cells and showed that inertia effects could provide a

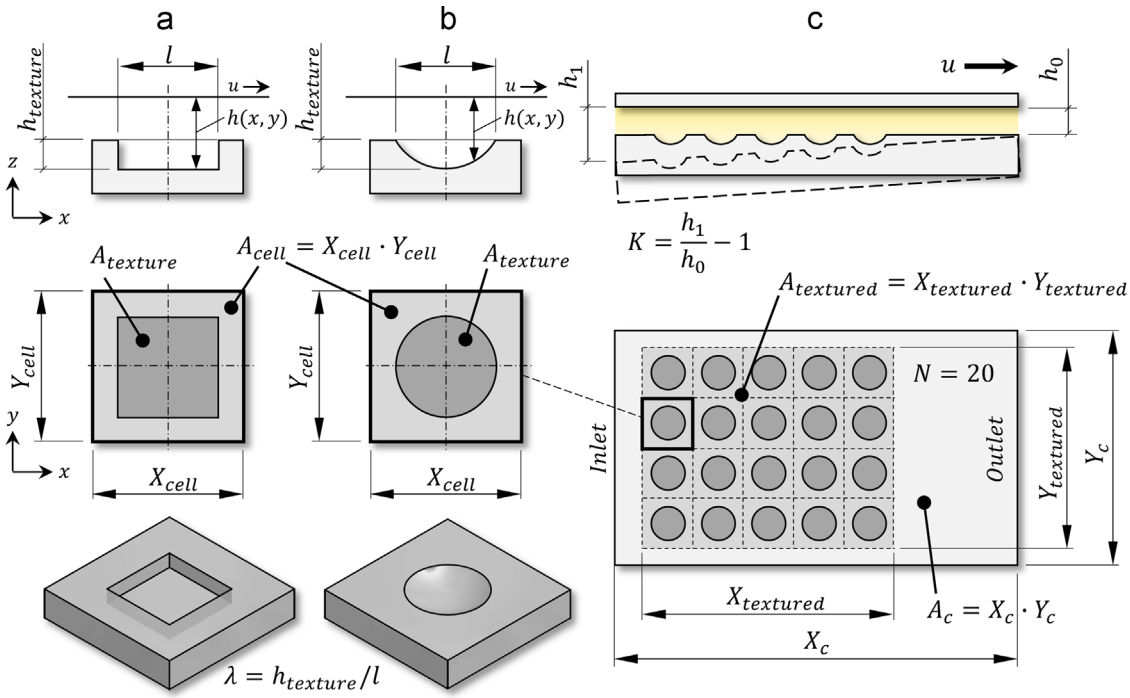

Fig. 4. Texturing parameters for parallel/convergent slider bearings: (a) Cuboid dimple with texture cell, (b) Spherical dimple with texture cell and (c) parallel/convergent slider bearing.

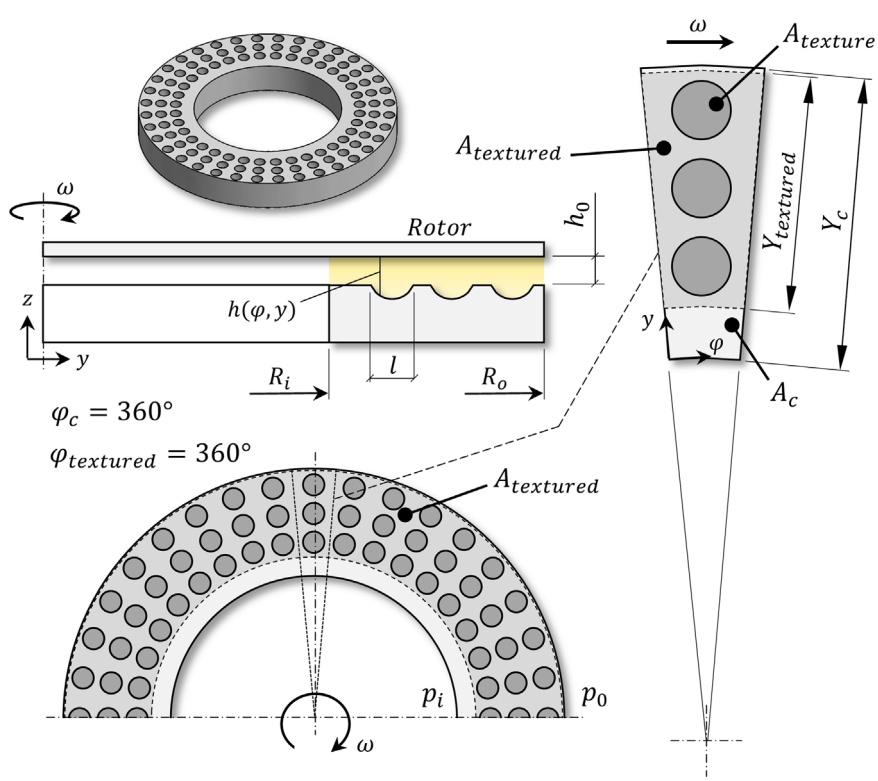

Fig. 5. Texturing parameters for seals and parallel rotating thrust bearings.

load carrying capacity for flows with higher Reynolds numbers. Note, however, that the considered dimple geometries had very large aspect ratios (λ) that are quite different from the ones typically studied in lubrication theory, leading to pronounced inertia effects. Subsequently, Sahlin et al. [66] further investigated inertia effects in single texture configurations using CFD and reported that the effects of inertia were the dominant mechanism for pressure build-up. In their study a maximum load carrying capacity could be achieved with a dimple depth close to the depth at which a vortex, i.e. flow recirculation within the dimple, appears. Completely contrary results were presented by Dobrica and Fillon in [67]. They studied the validity of the Reynolds equation for two-dimensional textured parallel slider configurations and concluded that inertia in general has a negative effect on the load carrying capacity.

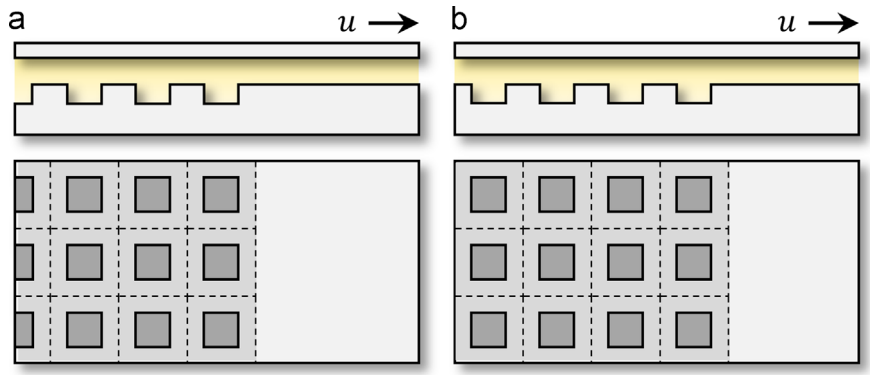

Fig. 6. (a) Partial texturing with shifted dimples and (b) Partial texturing with cell centred dimples.

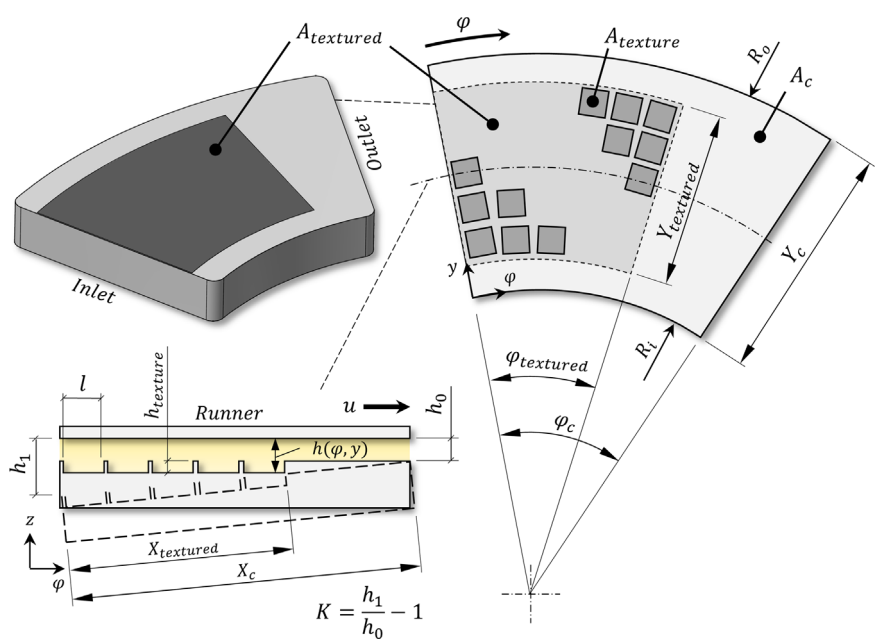

Fig. 7. Texturing parameters for parallel and convergent bearing pads.

De Kraker et al. [68] stressed that inertia can cause an increase or a reduction of the load carrying capacity, depending on the local flow conditions. More CFD investigations were carried out by Cupillard and co-workers for textured sliders [69–71] and journal bearings [72,73]. In [71] they also pointed out that inertia does not necessarily have positive effects on the load carrying capacity. In fact, positive influences were only observed up to a critical texture depth value, similar to the results by Sahlin et al. [66].

Another effect was described by Fowell et al. [61] and Olver et al. [60], as *inlet suction*, as mentioned above. They argued that the sub-ambient pressure caused by the diverging part of a single texture has the ability to *suck* more lubricant into the contact zone, hence increasing maximum pressure and load carrying capacity.

Yagi and Sugimura [74] suggested a mechanism called *balancing wedge action*. They studied the equilibrium of moment on a centrally pivoted pad bearing and concluded that the incorporation of a texture could disturb this balance, rotating the pad and thus increasing the convergence ratio. Hence, pressure and load carrying capacity could be generated by the resulting wedge action.

Etsion's group found that partial texturing can improve the tribological performance by a so-called *collective dimple effect*, similar to the concept proposed by Tønder [63,64]. They showed that the textured inlet has a larger average film thickness than the non-textured outlet and therefore a partially textured contact behaves similarly to a Rayleigh step bearing (see Fig. 3(d)–(f)). Note that the concept of partial texturing is a rather conventional way to create load support, as the hydrodynamic effects are caused solely by geometrically approximating a step or pocket. However, partial texturing can still have other advantages as compared to traditional stepped or pocketed contacts, e.g. act as lubricant reservoirs and trap wear debris. Fig. 3(f) shows typical pressure distributions over a stepped and partially textured slider. The pressure distribution over a partially textured slider is illustrated for three cases: (i) cavitation does not occur ($p_{cav} \ll p_{sup}$), (ii) cavitation occurs in the first two dimples ($p_{cav} < p_{sup}$) and (iii) cavitation occurs in all dimples ($p_{cav} = p_{sup}$). As long as $p_{cav} < p_{sup}$, significant pressure can build up, leading to a certain load support similar but inferior to the one encountered in stepped or pocketed contacts, even if cavitation does not occur at all. Therefore, cavitation cannot and should not be named as the responsible load support mechanism.

Etsion's group demonstrated the potential of partial texturing for mechanical seals [75], thrust bearings [19,36], journal bearings [15] and piston rings [76–78]. Partial texturing is generally considered more efficient than full texturing and often the only way to reasonably improve the tribological contact performance.

It is noteworthy that the aforementioned load-support mechanisms are complex phenomena that may occur simultaneously.

Moreover, the influence and magnitude of cavitation and inertia highly depend on the operating conditions and the type of contact. Hence, today's knowledge is that both phenomena may either improve or harm the overall contact performance, depending on the specific application.

3. Texture design

3.1. Texturing parameters

A slider bearing with circular/rectangular dimples is shown in Fig. 4 to illustrate the parameters commonly used to describe textured contacts. However, the parameters can easily be related to other textured components (see Figs. 5, 7 and 8).

An individual texture can be characterized by its three-dimensional shape (base shape and internal structure/bottom profile), size (base dimensions and depth) and in case of an asymmetric texture its orientation with respect to the direction of sliding. Another parameter that arises is the texture aspect ratio, which is defined as $\lambda = h_{texture}/l$, with $h_{texture}$ and l being the texture's maximal depth and dimension in sliding direction, respectively. In cases of circular textures l represents the texture's diameter. Although generally used in literature, this parameter does not capture the texture's base shape nor its internal structure.

On a global scale a textured contact can be further described by its relative textured portion $B = A_{textured}/A_c = \alpha \bullet \beta$ and its relative texture extends in x- and y-direction, given as $\alpha = X_{textured}/X_c$ and $\beta = Y_{textured}/Y_c$, respectively. To allow a consistent use of these parameters in this work, the relative texture extends are defined as $\alpha = \varphi_{textured}/\varphi_c$ and $\beta = Y_{textured}/Y_c$ in circumferential and radial direction, respectively, whenever polar coordinates are applied. The texture density ($\rho_{texture} = A_{texture}/A_{cell}$ for uniformly distributed textures or in general $\rho_{texture} = N \bullet A_{texture}/A_{textured}$, where N is the total number of textures) and the relative dimple depth $S = h_{texture}/h_0$ complete the parameters. Please note that in some literature a height ratio $H_r = (h_{texture} + h_0)/h_0 = S + 1$ rather than a relative dimple depth is used.

Although understandably all these parameters affect the overall contact performance, it is well accepted that dimple aspect ratio, texture density, relative dimple depth and for partial texturing, i.e. $A_{textured} \neq A_c$, the relative texture extends are the ones having the most pronounced influence and are thus the most important design parameters for textured contacts. Therefore most studies have been contributed to finding optimal values for those parameters.

3.2. Key findings for parallel contacts

3.2.1. Seals and parallel rotating thrust bearings

For the application of texturing in seals or seal-like structures, such as parallel rotating thrust bearings, the relative texture extend in circumferential direction $\alpha = \varphi_{textured}/\varphi_c$ is meaningless, because these contacts are obviously always fully textured in this direction, thus $\alpha = 1$ (see Fig. 5). Partial texturing in radial direction, however, can lead to high performance improvements for seals, as will be shown below.

The pioneering work on textured mechanical seals has been carried out by Etsion and co-workers. They conducted a series of theoretical parametric studies and experiments on face seals with dimples in the form of spherical caps ($5 \leq l \leq 200\ \mu m$ and $0 \leq \lambda \leq 0.5$) and found that textures can significantly improve seal performance and durability in terms of load carrying capacity, wear resistance, friction and face temperature [8,17,40,75]. They recommended a texture density of 20% and stressed that the dimple depth over diameter ratio λ can be optimized for given operating conditions and that this is the most important parameter. In [75] a seal was partially textured on the high pressure side, reassembling a virtual step in radial direction. An optimal value for the relative texture extend in radial direction was given in the range of $0.55 \leq \beta \leq 0.65$ in terms of average pressure. The experimental comparison of a partially textured seal with a smooth one showed a significant reduction in friction torque.

A mechanical gas seal, partially textured with elliptical dimples, was numerically investigated by Bai et al. [79]. They reported an open force improvement of 20% and demonstrated the importance of dimple orientation with respect to the direction of sliding.

Meng et al. [80] applied a Finite Element Method (FEM) with a mass-conserving cavitation algorithm to numerically investigate the influence of full texturing on a seal's flow rate and load carrying capacity. In their study texturing could not always increase the seal's load capacity, however, dimples were shown to be a feasible method to control seal leakage.

Brunetière and Tournerie [81] studied fully textured seals under mixed lubrication by solving the isothermal Reynolds equation together with a deterministic asperity contact model to incorporate roughness effects and a mass-conserving cavitation algorithm. In their investigation texturing was found to be incapable of generating any load carrying capacity whenever roughness effects of the untextured surface portions between textures were not considered. One the other hand, when roughness was accounted for, untextured and textured seals showed significantly better friction characteristics than smooth seals in both, mixed and hydrodynamic regime. These results stand in high contrast to previous findings for fully textured seals. The reason for this is the numerical treatment of cavitation: whereas many previous studies applied non-mass-conserving cavitation boundary conditions (Half-Sommerfeld or Reynolds) or did not consider cavitation at all, Brunetière and Tournerie used a mass-conserving approach based on the JFO boundary conditions, which correctly describes film rupture and reformation [82].

In fact, Ausas et al. [62] have shown that a non-mass-conserving treatment of cavitation highly overestimates the predicted load carrying capacity of dimpled surfaces and that therefore a mass-conserving implementation of cavitation is crucial in the field of surface texturing.

Following this new insight Qiu and Khonsari [58] further studied the effect of cavitation on fully textured rotating thrust bearings. In addition to experimentally observing local cavitation inside individual textures, they confirmed that a non-mass-conserving treatment of cavitation leads to a significant overestimation of load carrying capacity. It was concluded that for fully textured contacts load carrying capacity caused solely by cavitation is very limited. In a subsequent study by the same authors [38], a series of stainless steel rings (heat-treated 17-4 PH) were fully laser textured and experimentally evaluated. Samples with circular and elliptical dimples having different sizes ($200 \leq l \leq 2000\ \mu m$), depths ($46 \leq h_{texture} \leq 60\ \mu m$) and densities ($15 \leq \rho_{texture} \leq 58.6\%$) were considered. It was experimentally observed that at low speeds no cavitation occurs in the dimples, at increasing speeds gaseous cavitation and at high speeds vapor cavitation. Thus, cavitation pressure and therefore ultimately load carrying capacity is highly affected by the operational speed. Unlike the untextured specimens, which only showed minor scratches, the textured samples showed significant surface damage after conducting the aforementioned experiments. However, their coefficient of friction (COF) was considerably lower during all tests performed. It was further found that for a given dimple depth over diameter ratio λ, a higher texture density leads to higher friction reduction and for a given density an optimal value for λ exists.

In a later study Qiu and Khonsari [83] applied an averaged Reynolds equation to parametrically study fully textured thrust bearings considering roughness effects. It was shown that surface

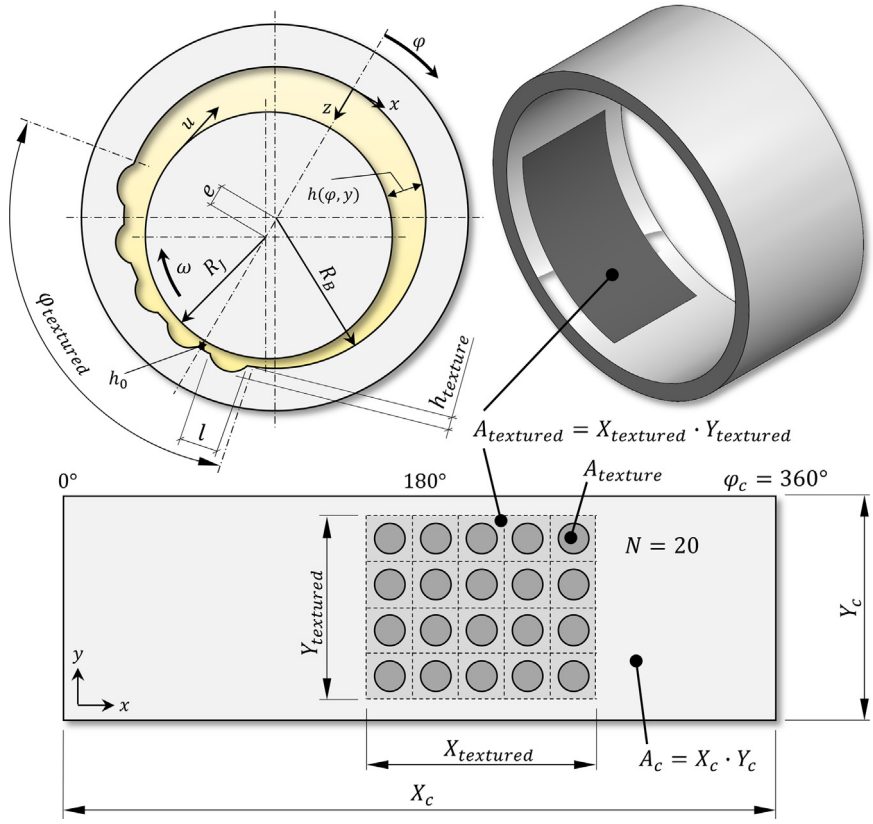

Fig. 8. Texturing parameters for journal bearings.

roughness has a positive but limited influence on bearing performance. They also found that optimal values for λ and $\rho_{texture}$ exist and that the cavitation pressure is crucial, which agrees well with findings in [17,84,38]. However, optimal texture parameters were found to highly depend on sliding speed and cavitation pressure.

Wang et al. [84] used reactive ion etching to produce circular dimples on SiC thrust bearings and in a series of experiments investigated the effect of different dimple sizes, depths and densities ($50 \le l \le 650$ μm, $2 \le h_{texture} \le 16.6$ μm and $0 \le \rho_{texture} \le 22.5\%$) on the load carrying capacity under water lubrication. All specimens in their study were fully textured. They illustrated the effect of texture density and depth over diameter ratio in a *load carrying capacity map* and stressed that both of these parameters can be optimized for given operating conditions. Optimal performance was achieved with the specimen having texturing parameters of $l = 350$ μm, $h_{texture} = 3.2$ μm and $\rho_{texture} = 5\%$. In a following study by the same group [85], the authors conducted further experiments with water lubricated SiC bearings having no textures, single-sized textures and mixed-sized textures. Interestingly, the rings having both, small and large dimples, showed the best performance, increasing load carrying capacity threefold when compared to the untextured specimen.

Zhang et al. [31] conducted pin-on-disc experiments with Babbitt alloy discs under mixed lubrication having circular dimples ($500 \le l \le 950$ μm, $h_{texture} = 10$ μm and $8.6 \le \rho_{texture} \le 13.9\%$) and stated that the lowest texture density studied (8.6%) gave the highest friction reduction.

In a very recent paper by Wang et al. [86], the authors reviewed published studies on the optimal texture density for fully textured contacts. They stressed that optimal texture densities stated in literature are usually much higher when predicted by theoretical methods than those obtained by experiments, as material properties are not accounted for. The authors recommended that texture densities should be in the range of $5 \le \rho_{texture} \le 13\%$ for oil lubricated metal components. Furthermore, a texture density exceeding 20% should be avoided to limit stress concentration effects.

The key findings for textured seals and seal-like structures, such as parallel rotating thrust bearings, can be summarized as follows:

- Full texturing may improve performance in terms of friction and load carrying capacity under certain conditions, however, reported performance improvements are usually very limited. Nevertheless, full texturing can be a feasible method to control seal leakage.
- Optimal values for λ and $\rho_{texture}$ for full texturing exist, but highly depend on operating conditions. Optimal densities given in literature are quite low and in a range between 5 and 20%.
- Roughness seems to have a positive but limited influence on the performance.
- A mass-conserving treatment of cavitation is crucial. Moreover, the ratio of cavitation over supply pressure (p_{cav}/p_{sup}) is an essential performance parameter.
- Partial texturing of seals in radial direction can lead to significant performance improvements by reassembling a virtual step. Optimal values for texture density, relative texture depth, texture aspect ratio and relative texture extend may be the ones most closely approximating an optimal step, as this seems to be the case for parallel slider bearings and parallel thrust pad bearings. However, studies in this direction are limited.

3.2.2. Parallel slider bearings and parallel thrust pad bearings

Parallel slider bearings and parallel thrust pad bearings are shown in Fig. 4 and 7, respectively. Especially for this type of contacts, texturing – in particular partial texturing – has shown to be highly beneficial and a reasonable way to improve contact performance.

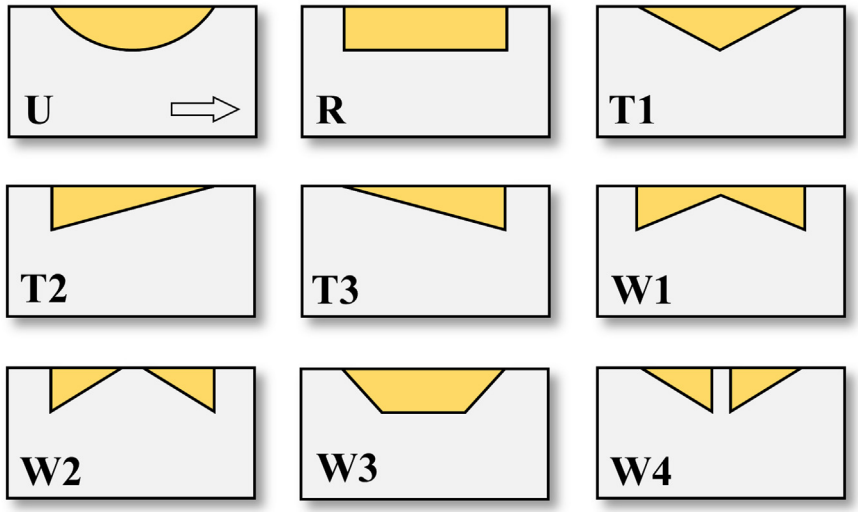

Fig. 9. Textures with different bottom profiles (adapted from [113]).

One of the first studies on textured parallel slider bearings was conducted by Brizmer et al. [19] in 2003. They numerically investigated bearing performance applying the two-dimensional Reynolds equation and found that whereas full texturing cannot provide a satisfying load support, partially textured contacts are capable of generating significant load carrying capacities. Parameters mostly affecting load capacity were found to be texture density, relative texture depth, relative texture extend and the bearing width to length ratio Y_c/X_c. Best performance enhancement was achieved with a relative texture extend in x-direction of 65%, a maximum possible texture density and a relative dimple depth of 1.25. The relative texture extend in y-direction was not investigated and kept constant at $\beta = 100\%$. Their findings were experimentally validated in a later study by the same group [36] by comparing non-textured and partially textured water lubricated parallel thrust pad bearings. The partial texturing resulted in a threefold increase in clearance and a friction reduction of 50%.

Following this study Rahmani and co-workers [87] attempted to find optimal texturing parameters with an analytical approach, applying the one-dimensional Reynolds equation for infinitely long parallel sliders having textures with flat bottom profiles. They stated optimal values for the relative texture depth in the range between 0.5 and 0.57 in terms of load capacity and friction force. It was further shown that a minimal number of textures results in best performance, which implicitly stands for a maximum texture density. In a more generalized optimization study by the same group [88], infinitely long parallel sliders with different texture bottom shapes were analysed. Three different bottom profiles were considered: R, T2 and T1 (see Fig. 9). The optimal value for the relative texture depth was found to be $S = 0.58$ for the flat textures (R) in terms of both, load carrying capacity and COF. For the other profiles, T2 and T1, values were found to be $S = 1.17$ and $S = 1.2$ for maximum load carrying capacity and minimum COF, respectively. In general, the performance of the flat textures (R) was reported to be superior.

Another analytical investigation on infinitely long parallel sliders was performed by Pascovici et al. [89]. They found optimal values for S and α to be in the ranges of $0.5-0.9$ and $50-62\%$, respectively, agreeing well with previous findings.

One of the first parametric numerical investigations on finite sliders was conducted by Dobrica et al. [10] in 2010, applying a two-dimensional mass-conserving form of the Reynolds equation. They demonstrated that fully textured parallel sliders can only generate load carrying capacities when the inlet is textured, i.e. textures are shifted towards the inlet in each cell, as shown for a partially textured contact in Fig. 6, but the effect was minimal. Note that texturing the inlet results in a larger inlet film thickness, which also means a higher oil supply rate is necessary. The question whether the term *full texturing* is still appropriate when the inlet is textured is debatable. On the other hand, partially textured parallel sliders were shown to be capable of creating substantial hydrodynamic lift, especially when the supply pressure is higher than the cavitation pressure ($p_{sup} > p_{cav}$) and textures are placed at the inlet. Furthermore, it was found that the texture density cannot be optimized for partially textured sliders, because load carrying capacity always increases with density, resulting in an optimum density of 100%. However, a density of 100% actually results in a stepped slider and the term *texture* becomes questionable. In practise, that means that the optimal texture density is the maximum achievable, limited by the fact that high densities may lead to stress concentration, weakening the surface.

Guzek et al. published unified computational approaches to optimize texturing parameters for both, two-dimensional [90] and three-dimensional [91] parallel slider bearings. Their results agreed well with findings of previous exhaustive analytical and numerical studies. For example, they also showed that increasing the texture density always leads to better performance and that shifting the textures towards the inlet is highly beneficial. Therefore the value for the texture density was set to 80% in their study. Optimal values for the relative texture depth were found to be $0.68 \leq S \leq 0.9$ for rectangular dimples and $0.97 \leq S \leq 1.21$ for elliptical dimples in terms of load carrying capacity. In terms of friction reduction optimal values were $0.76 \leq S \leq 0.81$ and $1.19 \leq S \leq 1.28$ for rectangular and elliptical dimples, respectively. The higher values obtained for elliptical dimples were explained by the fact that, as the volume of cuboid dimples is higher than that of ellipsoidal ones, cuboid dimples closer approximate a stepped bearing. This also confirms the results obtained by Rahmani [88]. The relative texture extend in x-direction was recommended to be 60% and in the range of $60-70\%$ for load carrying capacity enhancement and friction reduction, respectively, for both shapes.

Very recently Gherca et al. [92] published another numerical parametric study on three-dimensional textured parallel slider bearings. Whereas most results were quite similar to studies conducted by other researchers, they obtained much smaller optimal values for the relative texture extend in x-direction ($20 \leq \alpha \leq 40\%$ and $\beta = 100\%$). They also ran some simulations in transient flow conditions, i.e. the moving surface was textured

rather than the stationary one. Yet, the large computational power required limited the investigations to only a few geometric configurations. The results showed that texturing the moving surface instead of the stationary one may lead to a certain pressure build-up at the inlet, due to squeeze effects. However, texturing only the stationary surface was shown to be much more efficient. Interestingly, when both surfaces were textured, an additional performance improvement was obtained.

Malik and Kakoty [93] presented another parametric study on textured parallel sliders, however, their results are questionable as they used a non-mass-conserving cavitation algorithm. They concluded that for slider ratios of $Y_c/X_c = 2$ full texturing is preferable and for smaller ratios partial texturing is preferable.

Marian et al. [94] performed a thermo-hydrodynamic (THD) analysis of parallel thrust pad bearings with pads having rectangular dimples ($h_{texture} = 9\ \mu m$, $\lambda = 0.045$ and $\rho_{texture} = 25\%$) and found optimal relative texture extends of $\alpha = 50\%$ and $90\% \le \beta \le 100\%$ in terms of load carrying capacity maximization. These values are comparable to the ones obtained by other researchers.

A partially textured parallel eight-pad bearing (cuboid dimples, $l = 750\ \mu m$, $h_{texture} = 20\ \mu m$, $\alpha = 64\%$, $\beta = 75\%$ and $\rho_{texture} = 56\%$) was investigated by Charitopoulos et al. [95], solving the incompressible Navier–Stokes equations and considering thermal effects as well as elastic deformation. They stressed that oil heating significantly decreases the load carrying capacity of textured pad bearings, however, this is also the case for untextured bearings. A comparison of the relative influence of oil heating on the load carrying capacity between untextured and textured bearings was not conducted.

Henry and co-workers [37] experimentally compared smooth parallel thrust pad bearings with partially textured ones having rectangular dimples ($h_{texture} = 20\ \mu m$, $\lambda = 0.04$, $\alpha = 70\%$ and $\beta = 75\%$). At low loads texturing was able to reduce friction by up to 32% while at higher loads texturing was uninfluential or even detrimental. They also stated the importance of the position of the first row of textures relative to the pad inlet and that higher texture densities are preferable in terms of load carrying capacity, confirming previous findings by Dobrica et al. [10] and Guzek et al. [91].

Fouflias et al. [96] applied CFD to study four different bearing designs: open pocket, closed pocket, tapered-land and partially textured with rectangular dimples. Their results revealed that the textured bearing ($h_{texture} = 20\ \mu m$, $\lambda = 0.027$ and $\rho_{texture} = 56\%$) performs reasonable only at low and moderate rotational speeds. At high speeds its load carrying capacity is considerably lower compared to the other bearings, however, its friction torque is lowest in this case, because it shows the lowest values for minimum film thickness.

In a recent CFD study Papadopoulos et al. [23] proposed optimal relative texture extends for partially textured pad bearings having rectangular dimples ($h_{texture} = 20\ \mu m$, $\lambda = 0.027$and $\rho_{texture} = 56\%$). In their study highest load carrying capacity was obtained by texturing 2/3 and 3/4 of the pad length and width, respectively. Exact values for relative texture extents were given as $\alpha = 62\%$ and $75 \le \beta \le 85\%$. Furthermore, a relative dimple depth close to 1 was recommended, agreeing very well with findings from other researchers.

The key findings for parallel sliders and parallel thrust pad bearings can be summarized as follows:

- Full texturing can have detrimental or mild beneficial effects on the bearing performance, depending on operating conditions and cavitation phenomena. Beneficial effects have only been reported for certain cases, e.g. when the inlet is textured, and are very limited.
- Partial texturing on the other hand is capable of generating significant load support and reducing friction. Texturing the inlet is an efficient way to further increase load carrying capacity, as the higher inlet film thickness ensures sufficient lubricant supply for the first portion on the slider.
- The key to obtain best slider/pad performance seems to be to as closely as possible approximate an optimal step bearing. Optimal values obtained by different researchers are summarized in Table 1. For the step-bearing listed in Table 1, the relative texture extend in x-direction and the relative dimple depth stand for the relative inlet length and the relative step height ($(h_1 - h_0)/h_0$), respectively (see Fig. 3(d)). The best approximation can be achieved with rectangular textures having a flat bottom profile and a maximal possible texture density. Note, however, that a too high density may lead to stress concentration and thus increased wear or failure. The relative dimple depth should be just under 1 for rectangular dimples and slightly higher for other shapes.
- Studies are generally limited to unidirectional sliding conditions. More research needed regarding bidirectional conditions.

- Cavitation phenomena play an important role and influence contact performance. Particularly, an appropriate value of p_{cav} and the ratio of cavitation pressure over supply pressure is crucial [97]. Furthermore, cavitation should be taken into account in a mass-conserving way, when performing numerical simulations [62].
- Optimal texturing parameters are generally independent of speed and viscosity. However, changes in this values may result in the occurrence of cavitation, which can ultimately change optimal texturing parameters.

3.3. Key findings for non-parallel contacts

The more complex case of non-parallel applications, e.g. convergent sliding contacts or journal bearings, is less explored than the one of parallel contacts. In fact, the authors' literature survey revealed that about twice as many studies focused on parallel contacts. In the following the key findings for convergent contacts as well as journal bearings are reviewed.

3.3.1. Convergent contacts

Convergent contacts, such as plane inclined slider bearings (see Fig. 4) or tapered-land/tilting pad thrust bearings (see Fig. 7), are characterized by an overall wedge effect that in many cases overshadows any potential benefits from texturing. However, at low convergence ratios, K, textures may improve performance slightly, if designed correctly.

Cupillard et al. [70] studied infinitely long slider bearings having convergence ratios of 0.1, 0.2, 1 and 2 and relative texture depths of 0.1, 0.33 and 0.75 by solving the Navier–Stokes equations with a Finite Volume Method, without considering cavitation. For all these twelve cases considered, three dimples were

Table 1
Optimal texturing parameters given in selected literature for partially textured parallel sliders/pads.

Author	Reference	Y_c/X_c	α	β	S	$\rho_{texture}$
Brizmer et al.	[19]	1	60%	–	1.25	*max*
Rahmani et al.	[88]	∞	54…57%	–	0.58	*max*
Pascovici et al.	[89]	∞	50…62%	–	0.5…0.9	*max*
Dobrica et al.	[10]	1	–	100%	–	*max*
Guzek et al.	[91]	1	60…70%	–	0.68…0.9	*max*
Gherca et al.	[92]	0.6	20…40%	100%	–	*max*
Marian et al.	[94]	≈1	50%	90…100%	1	–
Papadopoulos et al.	[23]	≈0.8	62%	75…85%	≈1	*max*
Lord Rayleigh	[99]	∞	72%	–	0.87	100%

placed close to the slider inlet. The results showed that with respect to load carrying capacity texturing was more efficient at lower values of K. Moreover, it was found that optimal values for S highly depended on the convergence ratio. The authors further pointed out that flow recirculation may occur in deep dimples or close to the inlet at high convergence ratios, reducing load carrying capacity. The consideration of thermal effects in a later study [98] led to similar results.

The parametric investigation of Dobrica et al. [10] showed comparable results. It was shown that both, the gain of additional load carrying capacity and the reduction of friction decrease with an increase of convergence ratio, being best for $K=0$, which is the parallel case. It was further demonstrated that full texturing of convergent sliders is detrimental and partial texturing can lead to a small performance improvements. They also conducted a parametric optimization study to find optimal values (S, α and β) for convergence ratios in a range of $0.066 \leq K \leq 4$. The texture density was set to $\rho_{texture}=30\%$, as it was shown that increasing the density always leads to a better performance. This is also the case for partially textured parallel sliders, as discussed in the previous sections. The results revealed a high dependency of optimal values on the convergence ratio, except for the relative texture extend β, which remained 70% for a wide range of convergence ratios and reached a maximum of 100% for $K=0$. Optimal values for S and α were found to be in the ranges of $0.4 \leq S \leq 0.8$ and $0.4 \leq \alpha \leq 0.95$, respectively. The authors also proposed an additional performance enhancement by utilizing a trapezoidal shape for the textured region $A_{textured}$, similar to the concept of Aker's optimum finite Rayleigh step [99]. However, improvements were rather small.

Tønder [100,101] investigated fully textured pivoted plane bearings, applying the averaged Reynolds equation proposed by Patir and Cheng [102] and concluded that under certain conditions full texturing may improve friction, damping or stiffness, but in general full texturing is inefficient. However, these conclusions are very limited, as cavitation was not taken into account and only full texturing was considered.

Recently, Papadopoulos et al. [103] performed an optimization study applying genetic algorithms coupled with CFD to study optimal texturing parameters for three-dimensional inclined slider bearings having grooves perpendicular to the direction of sliding. The previous findings (i) maximal texture density always leads to best performance and (ii) texturing efficiency decreases with an increase in convergence ratio; could be confirmed in their study. They also demonstrated that optimal values for S and α highly depend on the slider's width to length ratio Y_c/X_c and convergence ratio, further confirming the findings in [10,70]. Equations providing optimal values of S and α for given Y_c/X_c and K were provided. Optimal partial texturing could improve load carrying capacity by up to 7.5% for low convergent sliders compared to the untextured configuration and pressure build-up was possible even for slightly divergent sliders. In a following study [104] the dynamic characteristics of optimal textured sliders were investigated. It was found that partially textured convergent sliders show improved stiffness but lower damping levels.

Fowell et al. [11] applied the Buckingham-PI theory to fully describe two-dimensional convergent slider bearings with just nine non-dimensional parameters. The importance and possible interactions of these parameters were then investigated in a parametric study. Their findings agree very well with those reported by other researchers and are not repeated here. However, their results first showed the complex interaction of different parameters. For example, it was observed that the sudden event of cavitation tends to disturb the otherwise continuous interaction between parameters, leading to complex but predictable relationships.

The following summarizes the key findings for convergent contacts:

- At convergence ratios close to 0, the summary given above for parallel sliders holds true.
- Full texturing of convergent contacts is detrimental and partial texturing can lead to mild performance improvements, however, only at low convergence ratios ($K<1$). At larger convergence ratios the influence of texturing diminishes completely.
- Optimal texturing parameters (α, β and S) highly depend on the convergence ratio and the slider's/pad's width to length ratio. Best performance is always achieved with a maximum possible texture density, i.e. the best configuration is actually a stepped/pocketed slider, as is the case for parallel contacts. As optimal values vary with K, textures designed for low convergence ratios may cause a performance degradation when used at high convergent ratios [10,11].
- Generally, cavitation effects are important, causing sudden changes on the performance and optimal texturing parameters. At higher values of K cavitation does not occur or is only present at small portions of the contact area, as the overall wedge effect builds up sufficient pressure to prevent pressures below p_{cav}. This was also shown in the CFD study by Brajdic-Mitidieri et al. [105].

3.3.2. Journal bearings

As the film thickness of a journal bearing in circumferential direction represents a converging-diverging gap (see Fig. 8), this application is probably the most challenging scenario in terms of surface texturing. The aforementioned may be responsible for the still limited number of publications on textured journal bearings. Another limitation is the large discretization effort encountered in the study of textured journal bearings. For example, in order to achieve an overall resolution of 5 μm for a journal bearing with diameter $D=100$ mm and width $Y_c=40$ mm, one would need a mesh containing about 500 million points.

One of the first studies on textured journal bearings was conducted by Tala-Ighil et al. [12] in 2007. They solved the two-dimensional Reynolds equation with a finite difference method, applying the Reynolds cavitation boundary condition to investigate the effect of spherical dimples on the bearing performance. It was shown that, depending on the dimple parameters (size, depth, density and distribution), texturing can have an either positive or negative influence on the main bearing characteristics (film thickness, load carrying capacity, axial flow rate and frictional torque) and thus, a proper texture design is crucial. In a later study by the same group [13] a journal bearing with cylindrical dimples ($h_{texture}=15$ μm, $l=2$ mm and $\lambda=0.0075$) was further investigated by means of numerical simulation, focusing on the effect of texture distribution. For this purpose 25 cases with the same textures but different texture distributions were simulated, including full texturing, partial texturing and a partial texturing of multiple zones of the bearing surface. They concluded that full texturing is ineffective, leading to a degradation in performance and that partial texturing including the texturing of multiple zones can be beneficial. Best performance was achieved when the area under the declining part of the pressure field was textured, although the improvements were minimal.

Ausas et al. [62] numerically investigated fully textured journal bearings with rectangular dimples with different texture depths. They reported a slight increase in minimum film thickness and friction torque due to texturing. It was furthermore shown that in the study of journal bearings, a mass-conserving treatment of cavitation is crucial, as the Reynolds cavitation model largely underestimates the cavitated area.

Cupillard et al. [72,73] simulated partially textured journal bearings using CFD and argued that deep textures ($S > 1$) should be located in the maximum pressure zone and shallow textures ($S \leq 1$) in the maximal film zone for high and low eccentricity ratios, respectively. They also observed a high dependence of optimal texturing values on the operating conditions and that the effect of texturing seems to be significantly higher at low eccentricities.

Brizmer and Kligerman [15] performed a non-dimensional parametric study on textured journal bearings. Their results showed that full texturing is inefficient and partial texturing can improve load capacity and attitude angle, however, reasonable improvement could only be observed at low eccentricity ratios, confirming the results obtained by Cupillard et al. [72,73]. Their results also showed a high dependency of optimal dimple depth and relative texture extend in circumferential direction on the bearing's eccentricity ratio.

Recently, Kango et al. [24,106] applied the Reynolds equation together with a mass-conserving cavitation algorithm to study journal bearings having spherical dimples or longitudinal/ transversal grooves. Temperature effects were considered by solving the energy equation simultaneously. It was found that partially texturing the convergent part of the bearing increases load carrying capacity compared to smooth and fully textured bearings. They further observed that texturing reduces the average temperature and that the performance improvement is more dominant at low eccentricity ratios, further confirming previous research in [15,72,73].

Lu and Khonsari [35] experimentally investigated fully and partially textured journal bearings with different dimple shapes and sizes ranging from $l = 2$ to 4 mm. Under mixed lubrication the fully textured bearing showed better performance than the partially textured one. They further stated that a careful design of texture size, shape and depth is crucial. Another experimental study was conducted by Dadouche et al. [34]. Four journal bearings were textured with equal spherical dimples ($h_{texture} = 60$ μm and $l = 1$ mm) but different texture densities and compared to an untextured bearing. The results revealed that texturing affects the dynamic bearing coefficients (stiffness and damping) and results in a slightly higher bearing temperature (+6–8 °C).

So far little research has been devoted to textured journal bearings and studies are limited to only certain scenarios. The findings so far are presented below:

- Full texturing is generally reported to be detrimental, however, contrary results have been obtained.
- Partial texturing can have beneficial effects, however, performance improvements have not been spectacular. The efficiency of texturing decreases with an increase in eccentricity ratio. This is similar to the case of convergent contacts, where a high convergence ratio overshadows the effects of texturing.
- In numerical simulations, cavitation effects should be treated in a mass-conserving way to avoid errors in the predicted performance.
- Optimal texturing parameters highly depend on operating conditions and eccentricity ratio. Furthermore, a wrong texture design can be counterproductive.

- The angular location of the textured area appears to be very important, however, very contrary results regarding the location have been reported and more research in this direction is needed.

3.4. Texture shape and internal structure

The two most commonly investigated dimple shapes are circular dimples with a curved bottom profile (spherical caps, see Fig. 4(b)) and rectangular dimples with a flat bottom profile (cuboids, see Fig. 4(a)). However, today's manufacturing techniques, e.g. laser surface texturing (LST) as the most commonly used one, are capable of producing all kinds of complex three-dimensional texture shapes (up-to-date reviews on different manufacturing techniques are given in [48,50]). Textures with different bottom profiles and base shapes are shown in Fig. 9 and Fig. 10, respectively, for example. A number of publications were devoted to study the effect of different texture shapes and internal structures on the performance of textured contacts.

Costa and Hutchings [33] experimentally investigated the influence of different geometries of surface textures on the hydrodynamic performance of sliding contacts. They performed a number of reciprocating sliding tests between stationary cylinders and fully textured sample plates with either grooves, circular or chevron-like dimples at different orientations, depths, densities and aspect ratios. A clear impact of texturing on the film thickness was observed. It was found that an optimal density exists for texturing with circular dimples and that out of all textures investigated ($\lambda \approx 0.1$), the one having a density of 11% resulted in the highest film thickness. Such an optimum was not observed for textures in the form of grooves, however, tests were limited to a

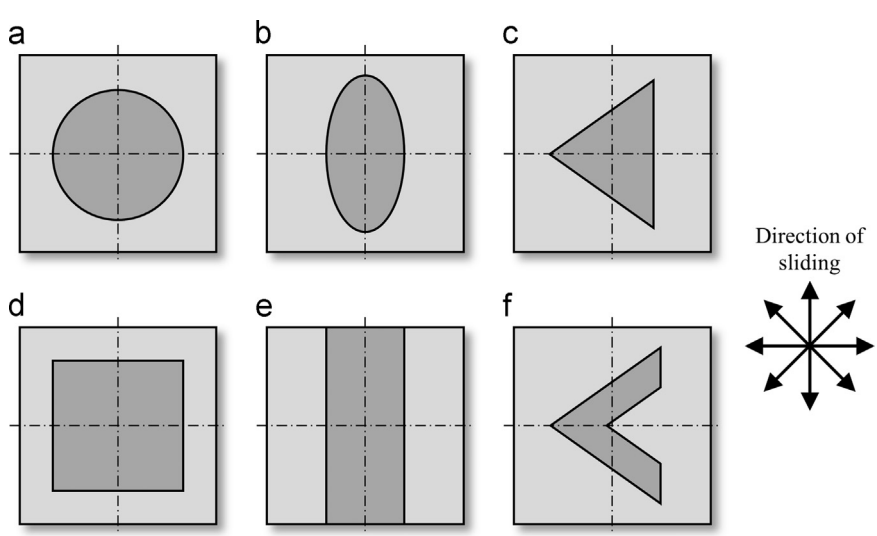

Fig. 10. Selection of different texture base shapes: (a) circular, (b) elliptical, (c) triangular, (d) rectangular, (e) groove and (f) chevron-like.

maximum density of 15%. The authors further stated that an optimal value for λ exists. In terms of texture orientation, chevrons pointing along the sliding direction were found to be most effective. This was explained by the restriction and direction of flow within a texture towards the high pressure side.

Yu et al. [107] studied the effect of different dimple shapes (circular, triangular and elliptical) and orientations on the pressure distribution. They simulated single texture cells applying the Reynolds equation with a non-mass-conserving treatment of cavitation (Reynolds) and periodic boundary conditions and concluded that the shape and orientation of dimples have a significant influence on the load carrying capacity. The best results were obtained with elliptical dimples having the major axis perpendicular to the direction of sliding. In their study all geometries had the same texture area $A_{texture}$, texture density and texture depth, which limits their conclusions, as individual shapes should be optimized before comparing them with each other, as stated by Etsion in [108]. In a later study by the same group [109], reciprocating sliding tests were carried out to further investigate the effect of dimple shape on the pressure generation. Circular, rectangular and elliptical dimples with different depths and densities were analysed and compared. It was found that individual shapes can be optimized for best performance and that elliptical dimples with the major axis perpendicular to the direction of sliding always showed the highest friction reduction under different load and speed conditions.

Qiu et al. [110] used the compressible form of the Reynolds equation to simulate the performance of gas-lubricated parallel slider bearings fully textured with six different dimple shapes (spherical, ellipsoidal, circular, elliptical, triangular and chevron-shaped). They optimized each shape individually before comparing them with each other and found that the ellipsoidal texture performed best in terms of load carrying capacity. They also stated that the base shape of the texture determines the optimal texture density whereas the optimal aspect ratio is defined by the dimple's internal structure. In a more recent paper [111], the authors also stressed that ellipsoidal dimples not only provide the minimal coefficient of friction, but also lead to highest bearing stiffness. Optimal texture density for this shape was found to be 35% and resulted in a 24.5% lower COF when compared to optimized circular textures. They further stressed that there exists an optimal geometry for every shape, however, this geometry is different depending on what the texture was optimized for: load carrying capacity maximization, friction reduction or stiffness maximization.

In a recent study, Shen and Khonsari [112] presented a numerical texture shape optimization approach based on the sequential quadratic programming (SQP) algorithm. They investigated fully textured parallel slider bearings and presented optimal dimple shapes for unidirectional sliding (chevron-like shapes with flat fronts) and bi-directional sliding (pairs of trapezoid-like shapes). They also compared the performance of these optimized shapes with textures having ordinary geometries (circle, ellipse, square, hexagon and diamond) and concluded that after optimization symmetric textures provide a higher load carrying capacity at a texture density of 30%, independently of operating conditions and cavitation pressure. However, at lower densities this superiority diminished. As they used a mass-conserving cavitation algorithm to simulate the regular shapes and a non-mass-conserving cavitation algorithm for the numerically optimized shapes, this comparison is questionable, as these different treatments of cavitation may lead to significantly different results [62].

The effect of different texture bottom profiles was explored in detail by Nanbu et al. [113] for concentrated conformal contacts applying an elasto-hydrodynamic lubrication (EHL) model (see Fig. 9). They found that textures with bottom profiles containing micro-wedges or micro-steps were able to further increase film thicknesses. Opposing results regarding the internal structure of textures were obtained by Shen and Khonsari in a recent paper [114]. They numerically and experimentally investigated the effect of circular dimples with different bottom profiles on the performance of parallel rotating discs and found that the flat profile yields the highest load carrying capacity.

The internal structure is also affected by the manufacturing technique itself. It is understandable that the real feature geometry may differ from the optimal and smooth shape usually considered in theoretical studies. Thus, in a study by Qiu and Raeymaekers [115] the effect of internal dimple-roughness was investigated. It was found that random Gaussian roughness inside a texture has a negligible impact on load carrying capacity, friction and flow rate. Charitopoulos et al. [116] further investigated manufacturing errors of grooves in thrust bearings using CFD. Deviations in texture shape, size and macroscopic errors, i.e. form errors of the contacting surfaces, were studied. It was found that in most cases these errors enhance load carrying capacity and improve friction characteristics.

Regarding texture shapes and internal structures it can be concluded that:

- Individual texture shapes can be optimized for given operating conditions.
- Asymmetric textures, e.g. ellipses and chevrons, seem to be the preferable option in terms of load carrying capacity enhancement and friction reduction, as they outperform the commonly used circular textures.
- An additional *tuning* of texture performance may be achieved by a careful selection of bottom profiles containing micro-steps, micro-wedges or both.
- Please note that the aforementioned findings are generally only valid for fully textured contacts. Partially textured contacts are an exception, as the best approximation of an optimal stepped or pocketed bearing always seems to be preferable, i.e. rectangular dimples with a flat bottom profile (cuboids) and maximal texture density.

Ultimately, universal guidelines on texture selection are impossible to give. Textures need to be carefully designed for a given type of contact and operating conditions. This further underlines the need for accurate and robust models that allow the evaluation of texture designs prior to being manufactured. The following is thus intended to provide a comparative summary of state of the art modeling techniques.

4. Modeling

Results of the authors' literature survey on modeling techniques used to analyse textured and/or rough surfaces are presented in Fig. 11. It can clearly be seen that the most common approach is the solution of the Reynolds differential equation with purpose-developed codes, usually with an easy implementable finite difference method, however, it will be shown here that this is not necessarily the best choice. Moreover, source codes are rarely provided, which has led to a variety of different models and contrary conclusions. This section is intended to provide a comparative overview of different available techniques to analyse textured and rough surfaces under hydrodynamic conditions.

4.1. Fluid mechanics

The motion of fluid is generally governed by the conservation equations for mass (Continuity equation) and momentum (Navier–Stokes equations). If gravitational and other external body forces

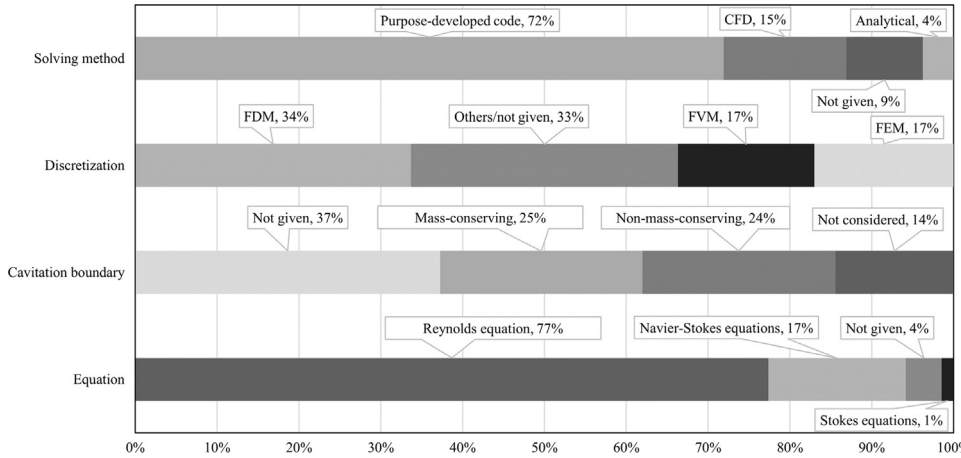

Fig. 11. Results of the literature survey on theoretical models for textured and rough surfaces.

are neglected and the flow is assumed to be Newtonian, steady and incompressible, the Continuity and Navier–Stokes equations in vector form can be written, respectively:

$$\nabla \bullet \boldsymbol{u} = 0 \tag{1}$$

$$\rho(\boldsymbol{u} \bullet \nabla)\boldsymbol{u} = -\nabla p + \nabla \bullet (\eta \nabla \boldsymbol{u}) \tag{2}$$

$\boldsymbol{u}$ is the velocity vector with the velocities u, v and w in x-, y- and z-direction, respectively, ρ the lubricant density, η the dynamic viscosity and p the pressure. The Stokes system of equations is formed by neglecting the convective inertia term (left-hand-side of equation (2)). Commonly used in lubrication theory is the classical Reynolds equation, derived by Osborne Reynolds in 1886 [117]. This partial different equation can be derived from the Navier–Stokes equations by neglecting inertia effects, body forces and assuming that the pressure gradient in film thickness direction is zero. Furthermore, all velocity gradients in x- and y-direction as well as $\partial w/\partial z$ are assumed to be zero. For a laminar and transient flow of an incompressible, isothermal and isoviscous lubricant, the Reynolds equation can be written as:

$$\frac{\partial}{\partial x}\left(h^3\frac{dp}{dx}\right) + \frac{\partial}{\partial y}\left(h^3\frac{dp}{dy}\right) = 6\eta u\frac{\partial h}{\partial x} + 12\eta\frac{\partial h}{\partial t} \tag{3}$$

where h is the film thickness, p the pressure, η the dynamic viscosity and u the velocity in sliding direction. Since, in most cases, no analytical solutions for any of these equations exist, a numerical solution is necessary. Whereas the Navier–Stokes or Stokes equations are usually solved with commercial CFD software or the *SIMPLE* algorithm, solutions of the Reynolds equation are generally obtained with purpose-developed codes.

The main advantage of the Navier–Stokes (NS) model lies in the more accurate and complete description of the flow, especially the ability to describe inertia effects and three-dimensional flow. On the other hand, the solution of the NS system of equations is much more time consuming. In particular, for simulations under transient conditions, parametric studies or whenever surface roughness or small textures are considered, a solution of the NS equations becomes impracticable. Thus, NS equations are often solved for small contact areas [70,71,118] or individual dimple configurations [65,66,119] to investigate texture lift-off phenomena in detail. However, some studies have been conducted for textured journal bearings [72,73] and thrust pad bearings [103,104,120]. Recently, CFD studies on thrust pad bearings were also extended to incorporate thermal effects by solving the Energy equation for both, the fluid and the solid domain [23,95,96].

One of the reasons for the popularity of the Reynolds equation is the lower computational effort required, as compared to the Navier–Stokes equations. Yet, due to the assumptions made during its derivation, the Reynolds equation is not capable of describing three-dimensional flow phenomena (e.g. recirculation inside textures) nor inertia related effects, which may lead to inaccurate results. The question whether the Reynolds equation or the Stokes equations are applicable for the study of textured surfaces has thus been the subject of numerous studies [66,121–123]. In 2009, Dobrica and Fillon [67] conducted an in-depth investigation on the validity of the Reynolds and Stokes models for textured slider contacts and demonstrated that the validity depends on two parameters: the Reynolds number (Re) and the texture aspect ratio (λ). It was shown that the Reynolds equation remains applicable as long as shallow dimples and flows with low Reynolds numbers are simulated. Deep textures may lead to recirculation, so that the Stokes system was recommended. For flows with high Reynolds numbers and whenever deep textures are studied, inertia and recirculation effects have a dominant influence on the pressure distribution and the full Navier–Stokes equations should be applied. They also showed that the applicability of the Reynolds equation can be largely improved by introducing correcting pressure terms to account for inertia based on the Bernoulli equation.

In summary, no consistent recommendation for the governing system of equations can be given. The choice depends on the specific application, operating conditions and texture configurations investigated. Despite the computational power available today, the Reynolds equation remains the more attractive choice in most cases, especially for more complex simulations involving, for example, transient conditions, rough surfaces or mixed lubrication. Whenever the Reynolds or Stokes equations are used, the validity should be evaluated for the application and range of operating conditions investigated. Please note that, since the Navier–Stokes equations are generally solved by commercial CFD software, the following sections are focused on methods based on the Reynolds equation.

4.2. Cavitation

In the study of textured or rough surfaces cavitation may occur not only globally in divergent contact areas, but also locally inside of individual dimples or in-between asperities (micro-cavitation) (see Fig. 12). As rupture and reformation of the lubricant film may occur multiple times, a mass-conservative treatment of cavitation has been shown to be crucial for accurate performance predictions [58,62]. A number of different mass-conserving cavitation algorithms have been proposed over the past 40 years. Developed algorithms are generally based on the well-accepted and experimentally validated JFO cavitation boundary conditions proposed

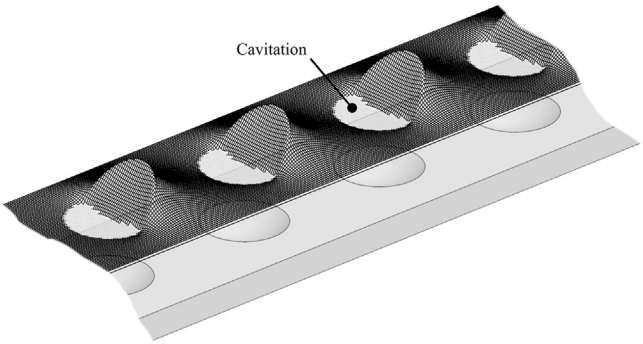

Fig. 12. Exemplary pressure distribution over a fully textured parallel slider with dimples in the form of spherical caps as predicted by the Reynolds equation and a mass-conserving treatment of cavitation.

by Jakobsson and Floberg [124] and Olsson [125] and many have been successfully implemented for the study of textured surfaces.

A first efficient cavitation algorithm that implicitly incorporates the JFO boundary conditions was developed by Elrod [126] and Elrod and Adams [127] in 1974. This algorithm is based on a Finite Difference Method (FDM) and iteratively divides the solution domain in a full film and cavitated region with the help of a switch function (g), defined as

$$g = \begin{cases} 0\theta < 1 \\ 1\theta \geq 1 \end{cases} \tag{4}$$

which also terminates the pressure terms in cavitated areas, allowing the use of a single equation throughout the domain and ensuring pure Couette flow in cavitated areas. Furthermore, a density ratio $\theta = \rho/\rho_c$ was introduced, which can also be interpreted as a fractional film content [126]. The flow in cavitated areas was treated as a two-phase flow of lubricant and vapor/gas with homogeneous density and in full film areas as a compressible flow with constant bulk modulus. The resulting modified Reynolds equation can be written as follows:

$$\frac{\partial}{\partial x}\left[\beta h^3 g(\theta)\left(\frac{d\theta}{dx}\right)\right] + \frac{\partial}{\partial y}\left[\beta h^3 g(\theta)\left(\frac{d\theta}{dy}\right)\right] = 6\eta u \frac{\partial \theta h}{\partial x} \tag{5}$$

where

$$\beta = \rho \frac{\partial p}{\partial \rho} \tag{6}$$

is the bulk modulus. Although the Elrod algorithm has been successfully applied in lubrication theory, the elliptic-hyperbolic character of this equation combined with the sudden changes in the switch function can lead to instability and may cause convergence problems [128]. Therefore, many improvements to the Elrod algorithm (also called $p-\theta$ algorithm) have been proposed hereafter.

In 1986, Brewe [129] applied the $p-\theta$ model to study dynamically loaded journal bearings. As the Elrod algorithm requires and iterative solution, he used an alternating direction implicit (ADI) method and in a later study together with Woods [130] Multigrid techniques to increase convergence speed. Vijayaraghavan and Keith [131,132] modified the Elrod algorithm some years later by using different finite difference schemes for the two flow regions, which improved its numerical stability. Their model was applied, for example, for textured thrust bearings by Qiu and Khonsari [58], using a Multigrid method with an iterative Gauss–Seidel relaxation scheme based on FDM. In a later study by the same authors [83], the algorithm was applied together with the Patir and Cheng (P&C) flow factor method to study roughness effects inside textures.

In 1991, Kumar and Booker [133,134] proposed an algorithm for transient conditions optimized for FEM. Their algorithm was recently successfully applied by XIE et al. [135] for textured surfaces considering roughness effects. Other models based on FEM were developed by, for example, Shi and Paranjpe [136] and Hajjam and Bonneau [137]. The model of [137] was recently applied for the study of textured parallel sliders under steady and transient conditions by Gherca et al. [92].

Another cavitation algorithm was developed by Payvar and Salant in 1992 [138]. Based on the $p-\theta$ theory, they developed a finite difference version of the algorithm with optimized numerical stability. Their model was adapted for mixed lubrication by Wang et al. in 2003 [139], applying the P&C flow factor method and a rough surface contact model to study misalignment effects in coupled journal-thrust bearings. Harp and Salant [140] made use of the Payvar–Salant algorithm to develop a universal Reynolds equation that allows a simultaneous calculation of macro and micro-cavitation in rough journal bearings. The Payvar–Salant algorithm was also successfully applied for the study of lip seals under mixed lubrication [141], textured thrust bearings [59] and textured rough seals [81]. Recently, Xiong and Wang [142] performed a detailed analysis of the numerical finite volume implementation of this model, in particular regarding different finite difference schemes and solvers.

In 2007, Sahlin et al. [143] proposed an iterative algorithm based on a FDM that incorporates a switch function, similar to the concept of Elrod. However, rather than using an explicit relation between pressure and density based on the bulk modulus, their model allows an arbitrary treatment of compressibility. Fesanghary and Khonsari [128] proposed another improvement to the Elrod algorithm. They used a continuous switch function (g) instead of the conventional binary one and reported significant improvements in numerical stability and convergence speed.

Ausas et al. [62] proposed a finite volume based version of the $p-\theta$ model for incompressible fluids. The arising nonlinear system of equations was solved with an iterative Gauss–Seidel method with successive over-relaxation. In 2009, the same group published a transient version of their cavitation algorithm and applied it for dynamically loaded journal bearings and squeeze flows [144]. It is noteworthy that their source code is publicly available on the internet. Their algorithm was applied, for example, in the numerical texture-optimization study by Guzek et al. [91], considering thermal effects by simultaneously solving the Energy equation, and for piston ring/cylinder liner contacts by Spencer et al. [145] in 2011.

Recently, Giacopini et al. [146] took advantage of the mathematical concept of complementarity used in the study of free boundary problems. After reformulating and discretizing the Reynolds equation through FEM, they constructed a linear complementarity problem (LCP) for which well-developed solution techniques exist that result in a converged solution within a finite number of steps. Bertocchi et al. [147] extended this model to include compressibility, piezoviscosity and non-Newtonian fluid behavior. The model was applied recently by Medina et al. [148] to study textured bearings under transient reciprocating conditions.

To evaluate the stability and convergence characteristics of some of today's most sophisticated cavitation models, Woloszynski et al. [148] compared required iterations and computation times of the algorithms proposed by Ausas et al. [144], Bertocchi et al.[147] and Fesanghary and Khonsari [128] with their own algorithm based on a LCP formulation, called Fischer–Burmeister–Newton–Schur (FBNS). In their paper from 2015, fully textured parallel sliders having different numbers of dimples and different mesh densities were considered. The results showed that the proposed FBSN model is significantly faster (two orders of magnitude) than the other algorithms. The algorithm developed by

Bertocchi et al. only converged within reasonable time when very coarse grids were used. The algorithms by Ausas and Fesanghary/Khonsari both always converged, the latter being about twice as fast on average. The truly impressive superiority of their algorithm was further demonstrated for textured contacts under transient conditions.

A variety of solutions to the complex task of solving the arising system and determining priori unknown cavitation zones within the solution domain have been proposed. Algorithms were optimized for different discretization methods, modified for improved stability or enhanced computational efficiency and incorporated in the study of rough surfaces, mixed lubrication, transient flow and thermo-hydrodynamic lubrication. However, no easily implementable standard method exists and numerical details or source codes are rarely provided, hence, the often time-consuming implementation remains with the individual researcher. This inevitable leads to slightly different algorithms and makes comparison and validation difficult. The question of which algorithm should be applied depends on the specific problem investigated. Especially for the simulation of transient conditions or whenever very small meshes are required, more computational efficient algorithms (e.g. [149]) may become necessary, despite the generally more complex implementation.

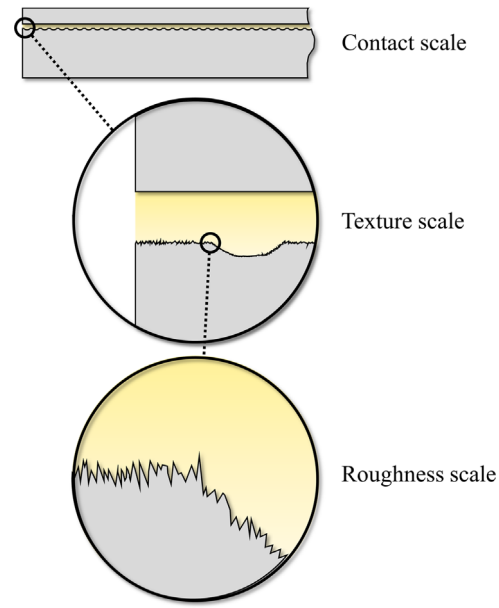

Fig. 13. Different scales of a textured contact.

4.3. Micro-hydrodynamic

Another issue in the simulation of textured surfaces is the large difference in scale between the global contact dimensions and local surface properties, such as textures or roughness (see Fig. 13). Generally, two different approaches exist to consider these local changes in film thickness in the numerical solution: direct/deterministic methods and indirect/stochastic methods.

In the direct method the mesh is chosen fine enough to capture the surface topography up to the micro/nano-scale, i.e. roughness and/or textures are directly included in the film thickness equation. This may work for medium-sized and large textures, however, if textures are very small or one wants to consider the effect of surface roughness, a direct method becomes nearly impossible due to the fine meshes needed and the related high computation time encountered. Only for very small domains, e.g. Hertzian contacts, this method becomes applicable. The EHL contact model by Hu and Zhu [150,151], for example, was used to deterministically investigate differently engineered surfaces, including dimpled ones, by Epstein et al. [152], Wang and Zhu [153] and Wang et al. [154]. Brunetière and Tournerie [81] were able to deterministically investigate fully textured seals while considering roughness by reducing the solution domain with the help of periodic boundary conditions. Other proposed deterministic models include those by Shi and Salant [141] and Jiang et al. [155].

Despite the advantages in accuracy, a direct method can rarely be applied, which has led to the development of numerous indirect/stochastic methods. All these methods include some kind of averaging and can be divided into two groups: flow factor methods and homogenization methods.

In flow factor methods the influence of local changes in film thickness on the pressure distribution is incorporated in the pressure and shear flow terms of the Reynolds equation by a number of correction factors, so-called *flow factors*. One of the earliest and most popular methods is the P&C flow factor method, developed in 1978 by Patir and Cheng [102,156]. The steady-state form of the P&C averaged Reynolds equation can be written as:

$$\frac{\partial}{\partial x}\left(\phi_x h^3 \frac{dp}{dx}\right) + \frac{\partial}{\partial y}\left(\phi_y h^3 \frac{dp}{dy}\right) = 6\eta u \frac{\partial h}{\partial x} + 6u\sigma \frac{\partial \phi_s}{\partial x} \tag{7}$$

where ϕ_x and ϕ_y are pressure flow factors, ϕ_s is the shear flow factor and σ the surface rms roughness. Pressure flow factors are generally obtained through numerical experiments performed on a local scale, i.e. a small representative contact area, and ϕ_s was given in [156]. Despite numerous proposed improvements and modifications (see e.g. Elrod [157], Tripp [158], Wu and Zheng [159], Harp and Salant [140], Rocke and Salant [160] or Wilson and Marsault [161]), the classic P&C method is still the most commonly used flow factor technique in the study of textured/rough surfaces and was applied, for example, in the study of journal bearings with axial grooves by Chan et al. [162], dimpled contacts by XIE [135] and textured bearings by Tønder [100,101].

Especially for the study of textured contacts, de Kraker et al. [68,163] developed a *texture averaged Reynolds equation*. Similar to the P&C theory, so-called *texture flow factors* were introduced to modify the Reynolds equation on the global domain. Unlike in Patir and Cheng's method, flow factors were obtained by local flow simulations based on the Navier–Stokes equations rather than the Reynolds equation in order to account for inertia and recirculation effects and depend on the operating conditions. In 2006, Dobrica et al. [164] compared the results obtained by the P&C flow factor model with a deterministic model for a partial arc journal bearing. It was found that, in general, the P&C model showed a good agreement with the deterministic results in terms of pressure and film thickness, although values for friction torque and attitude angle showed deviations.

The other type of indirect method is based on the mathematical concept of homogenization, used for partial differential equations (PDEs) with oscillating coefficients. Similar to the aforementioned flow factor techniques, multiple scales are used and local effects are averaged and then incorporated in the global, smooth Reynolds equation. The due to surface roughness or textures oscillating film thickness equation is homogenized, resulting in a so-called *homogenized Reynolds equation*. This method was originally proposed by Elrod [165] in 1973 and has been further studied by many authors [164,166–177].

For example, Bayada et al. [169] proposed a homogenized Reynolds equation that incorporates mass-conserving cavitation based on the JFO boundary conditions and Sahlin et al. [175,176] developed a mixed lubrication model that allows the simulation of measured surface topography. Another interesting concept based on homogenization was applied by Almqvist et al. [177], called *reiterated homogenization*. They studied the combined effect of

surface roughness and texturing by dividing the problem in three scales rather than two: a roughness scale, a texture scale and the global contact scale. Both, the oscillations of the roughness and texture scale were homogenized and incorporated in the global, smooth Reynolds equation. Since the study of rough textured surfaces involves three scales, one could also treat the texture scale deterministically and the roughness scale with a homogenization or flow factor method, resulting in a *semi-deterministic* approach, as performed by Spencer et al. [145] for textured cylinder liners and by Qiu and Khonsari [83] for seal-like structures.

It has been shown that, compared to classic flow factor methods, the concept of homogenization leads to more accurate results whenever arbitrary roughness is encountered, i.e. the patterns do not show any symmetries [175–177]. Hence, for cases with arbitrary roughness patterns the homogenization techniques is recommended.

Generally, it should be noted that local flow information is lost whenever stochastic methods are used, hence, a deterministic method is always preferable, particularly for textures, as local cavitation has an important influence on the contact performance. Also, partially textured contacts would require locally different flow-factors. The same holds true for surface roughness, however, a deterministic treatment is, despite the available computational power today, not usually applicable and therefore some kind of averaging technique needs to be performed.

4.4. Spatial discretization and numerical methods

In most cases, the Reynolds equation requires a numerical solution, i.e. a discretization of the solution domain and a subsequent solution of the arising systems of algebraic equations. Generally, mathematics provides methods for the solution of this type of equation and the reader is referred to respective literature. However, some issues arise particularly in the study of textured surfaces and are briefly discussed here.

The Reynolds equation is an elliptic second order PDE, however, whenever mass-conserving cavitation is considered, the equation becomes hyperbolic in cavitated areas, forming a highly nonlinear mixed type PDE. Most discretization methods are applicable for this kind of equation and many have been successfully applied in the field of surface texturing (e.g. see: Finite Difference Method (FDM) [58,108,128,178,179], Finite Volume Method (FVM) [10,91,142,178–180], Finite Element Method (FEM) [137,146,178,179], Finite Cell Method (FCM) [181] and Spectral Element Method (SEM) [178,179]).

One of the differences between these methods is their capability of handling discontinuous coefficients. As surface textures in the form of dimples or grooves are discontinuities in the film thickness equation by nature, special care should be taken regarding discretization and meshing. For methods based on finite elements this issue is less pronounced, since the element edges can be made coincide with the discontinuities [92,182,183]. For FDM and FVM, on the other hand, discontinuities may cause large approximation errors, especially in cavitated areas, since the hyperbolic type of the Reynolds equation does not allow the use of central finite difference schemes. Thus, whenever the discretization is based on finite differences, a special treatment of discontinuities is generally required, such as local mesh refinement [184] or special finite approximation schemes [182,185].

Also, the accuracy and convergence speed of the solution may differ, depending on the discretization method chosen. Recently, Woloszynski et al. compared the accuracy of four different discretization methods (FDM, FVM, FEM, SEM) for one-dimensional [178] and two-dimensional [149] textured slider bearings. It should be noted here that, since cavitation was not considered in their study, the problem considered was purely elliptic. The number of mesh points required in order to achieve a predetermined accuracy was evaluated for each method and compared. SEM was shown to require the smallest number of nodes, 28 and 72 times fewer than the other methods for the one-dimensional and two-dimensional case, respectively, resulting in a significantly higher convergence speed. Both, FVM and FEM were stated to be the best compromise between accuracy and ease of implementation. FDM required the highest number of nodes and was not recommended. Nevertheless, due to the ease in implementation, FDM is the most popular discretization method used in the study of textured surfaces (see Fig. 11), despite its inaccuracy and inability to handle complex geometries.

The generally fine meshes required to accurately describe surface textures and the complexity of the Reynolds equation especially related to cavitation phenomena require fast and robust solvers. The choice of the numerical solver obviously depends on the numerical details of the model and the particular system of equations encountered after discretization. For example, a number of cavitation algorithms are iterative by design and, thus, require iterative solvers. Very popular in the study of surface textures are Gauss–Seidel methods, often implemented with successive relaxation (see e.g. [10,12,62,128,149]) to improve convergence speed. Other successfully applied iterative schemes include alternating direction implicit (ADI) methods [160] and for nonlinear systems Newton–Raphson [186,187] methods. Cavitation algorithms based on LCP can take advantage of pivoting algorithms [146–149, 188], for example, Lemke's algorithm [189]. Also, in order to further increase convergence speed, Multigrid methods [58,83,112,114] have been applied and algorithms were modified to take advantage of multicore processing [25,162].

5. Limitations of this review

This review is focused on findings regarding texturing for typical bearing applications under hydrodynamic conditions. Texture design choices may differ for counterformal contacts or other lubrication regimes. For research on surface texturing for concentrated contacts the reader is referred to a recently published review article by Sudeep et al. [45] and for studies concerning different lubrication regimes the reader may be interested in references [26,27,29,56].

The review on modeling techniques presented in this paper is focused on methods based on the Reynolds equation and is limited to hydrodynamic lubrication, cavitation and micro-hydrodynamic effects. If the reader is interested in the simulation of mixed lubrication or elasto-hydrodynamic modeling, references [47,190–192] may be interesting. Furthermore, it is well known that thermal effects and elastic deformation play a crucial role in hydrodynamic lubrication, particularly in bearings, and these effects should be included in the numerical simulation for accurate performance predictions. Also, whenever the Reynolds equation is applied, additional models to describe turbulent flow may become necessary for certain applications. However, these effects were not considered *texture-specific*, and have thus not been included in this review. Temperature effects have been included in the theoretical study of textured surfaces based on the Reynolds equation by a simultaneous solution of the Energy equation. The interested reader is referred to references [24,91,94,106].

6. Concluding remarks

Surface texturing has been shown to be capable of enhancing the tribological contact performance for a wide range of applications. One of the main issues is the dependency of optimal

texturing parameters on the type of contact and, in particular, the operating conditions. Furthermore, complex phenomena, such as cavitation and inertia related effects, have been shown to highly affect texture performance.

A lot of research has thus been aimed at finding optimal texturing parameters for best performance enhancement. Although some general guidelines exist, it has become clear that in most cases textures need to be designed for a specific application and given operating conditions. Especially for convergent film geometries or journal bearings, for which optimal parameters have been shown to significantly depend on the convergence ratio or the eccentricity, the chosen texture design will always be a compromise, adapted for the range of operating conditions encountered. For some scenarios texturing may even be found to be detrimental or provide unreasonable improvements; this means that the profitability and effectiveness of surface texturing need to be assessed for a given application.

Robust numerical models allow the evaluation of texture designs prior to being manufactured and can avoid time consuming experimental trial and error approaches. Although a range of theoretical models have been developed and applied for textured surfaces, the numerical study still involves three major challenges: (i) a mass-conserving treatment of cavitation has been shown to be crucial, however, the arising elliptic-hyperbolic system with initially unknown locations of cavitation areas provides difficulties and may lead to numerical instabilities. (ii) Surface textures are discontinuities in film thickness by nature. To avoid errors, a special handling of these discontinuities is required during discretization. (iii) The large difference in contact and texture dimensions often results in very fine meshes and therefore impractical computation times. Especially when roughness is considered, averaging techniques need to be applied, which lead to the loss of local flow information. Additionally, the assumptions made by using the Reynolds equation may be violated, depending on the Reynolds number and texture dimensions. Hence, the applicability of the Reynolds equation should be evaluated for all simulations performed.

Surface texturing remains a feasible method for contact performance enhancement in terms of load carrying capacity, minimum film thickness, friction and wear. Robust models are crucial for a successful application, however, the lack of publicly available implementation details has led to a large variety of different numerical models, which makes it difficult to compare results and develop new and improved codes, especially for new researchers in the field. Public availability of source codes is an important step towards standard techniques and ultimately robust and accurate models that will facilitate and extend the applicability of this technology.

Acknowledgments

The authors acknowledge the financial support of the Engineering and Physical Sciences Research Council (EPSRC) via grant EP/M50662X/1.

References

[1] Bhushan B. Biomimetics: lessons from nature – an overview. Philos Trans R Soc Lond A: Math Phys Eng Sci 2009;367:1445–86.
[2] Dean B, Bhushan B. Shark-skin surfaces for fluid-drag reduction in turbulent flow: a review. Philos Trans R Soc A: Math Phys Eng Sci 2010;368:4775–806.
[3] Jearl W. More on boomerangs, including their connection with the dimpled golf ball. Sci Am 1979:180.
[4] Hamilton DB, Walowit JA, Allen CM. A theory of lubrication by microirregularities. J Fluids Eng 1966;88:177–85.
[5] Anno JN, Walowit JA, Allen CM. Microasperity lubrication. J Tribol 1968;90:351–5.
[6] Anno JN, Walowit JA, Allen CM. Load support and leakage from microasperity-lubricated face seals. J Tribol 1969;91:726–31.
[7] Willis E. Surface finish in relation to cylinder liners. Wear 1986;109:351–66.
[8] Etsion I, Burstein L. A model for mechanical seals with regular microsurface structure. Tribol Trans 1996;39:677–83.
[9] Etsion I. State of the art in laser surface texturing. J Tribol 2005;127:248–53.
[10] Dobrica MB, Fillon M, Pascovici MD, Cicone T. Optimizing surface texture for hydrodynamic lubricated contacts using a mass-conserving numerical approach. J Eng Tribol 2010;224:737–50.
[11] Fowell MT, Medina S, Olver AV, Spikes HA, Pegg IG. Parametric study of texturing in convergent bearings. Tribol Int 2012;52:7–16.
[12] Tala-Ighil N, Maspeyrot P, Fillon M, Bounif A. Effects of surface texture on journal-bearing characteristics under steady-state operating conditions. Proc Inst Mech Eng Part J: J Eng Tribol 2007;221:623–33.
[13] Tala-Ighil N, Fillon M, Maspeyrot P. Effect of textured area on the performances of a hydrodynamic journal bearing. Tribol Int 2011;44:211–9.
[14] Kango S, Singh D, Sharma RK. Numerical investigation on the influence of surface texture on the performance of hydrodynamic journal bearing. Meccanica 2012;47:469–82.
[15] Brizmer V, Kligerman Y. A laser surface textured journal bearing. J Tribol 2012;134:031702.
[16] Kango S, Sharma RK. Studies on the influence of positive roughness on the performance of journal bearing. J Tribol Surf Eng 2010;1:243–62.
[17] Etsion I, Kligerman Y, Halperin G. Analytical and experimental investigation of laser-textured mechanical seal faces. Tribol Trans 1999;42:511–6.
[18] Razzaque MM, Faisal MTR. Performance of mechanical face seals with surface micropores. J Mech Eng 2007:37.
[19] Brizmer V, Kligerman Y, Etsion I. A laser surface textured parallel thrust bearing. Tribol Trans 2003;46:397–403.
[20] Fesanghary M, Khonsari MM. On the optimum groove shapes for load-carrying capacity enhancement in parallel flat surface bearings: theory and experiment. Tribol Int 2013;67:254–62.
[21] Mezghani S, Demirci I, Zahouani H, Mansori ME. The effect of groove texture patterns on piston-ring pack friction. Precis Eng 2012;36:210–7.
[22] Zhou Y, Zhu H, Tang W, Ma C, Zhang W. Development of the theoretical model for the optimal design of surface texturing on cylinder liner. Tribol Int 2012;52:1–6.
[23] Papadopoulos CI, Kaiktsis L, Fillon M. Computational fluid dynamics thermohydrodynamic analysis of three-dimensional sector-pad thrust bearings with rectangular dimples. J Tribol 2014;136 (011702-1-10).
[24] Kango S, Sharma RK, Pandey RK. Thermal analysis of microtextured journal bearing using non-Newtonian rheology of lubricant and JFO boundary conditions. Tribol Int 2014;69:19–29.
[25] Han Y-F, Chan C-W, Wang Z, Shi F, Wang J, Wang N, et al. Effects of shaft axial motion and misalignment on the lubrication performance of journal bearings via a fast mixed EHL computing technology. Tribol Trans 2015;58:247–59.
[26] Kovalchenko A, Ajayi O, Erdemir A, Fenske G, Etsion I. The effect of laser texturing of steel surfaces and speed-load parameters on the transition of lubrication regime from boundary to hydrodynamic. Tribol Trans 2004;47:299–307.
[27] Podgornik B, Vilhena LM, Sedlacek M, Rek Z, Žun I. Effectiveness and design of surface texturing for different lubrication regimes. Meccanica 2012;47:1613–22.
[28] Scaraggi M, Mezzapesa FP, Carbone G, Ancona A, Tricarico L. Friction properties of lubricated laser-microtextured-surfaces: an experimental study from boundary- to hydrodynamic-lubrication. Tribol Lett 2013;49:117–25.
[29] Braun D, Greiner C, Schneider J, Gumbsch P. Efficiency of laser surface texturing in the reduction of friction under mixed lubrication. Tribol Int 2014;77:142–7.
[30] Scaraggi M, Mezzapesa FP, Carbone G, Ancona A, Sorgente D, Lugarà PM. Minimize friction of lubricated laser-microtextured-surfaces by tuning microholes depth. Tribol Int 2014;75:123–7.
[31] Zhang H, Zhang DY, Hua M, Dong GN, Chin KS. A study on the tribological behavior of surface texturing on babbitt alloy under mixed or starved lubrication. Tribol Lett 2014;56:305–15.
[32] Wang W, Huang Z, Shen D, Kong L, Li S. The effect of triangle-shaped surface textures on the performance of the lubricated point-contacts. J Tribol 2013;135:021503-.
[33] Costa HL, Hutchings IM. Hydrodynamic lubrication of textured steel surfaces under reciprocating sliding conditions. Tribol Int 2007;40:1227–38.
[34] Dadouche A, Conlon M, Dmochowski W, Koszela W, Galda L, Pawlus P. Experimental evaluation of steady-state and dynamic performance of hydrodynamic journal bearings: plain versus textured surface. 10th EDF/Pprime workshop. Poitiers, France; 2011.
[35] Lu X, Khonsari MM. An experimental investigation of dimple effect on the stribeck curve of journal bearings. Tribol Lett 2007;27:169–76.
[36] Etsion I, Halperin G, Brizmer V, Kligerman Y. Experimental investigation of laser surface textured parallel thrust bearings. Tribol Lett 2004;17:295–300.
[37] Henry Y, Bouyer J, Fillon M. An experimental analysis of the hydrodynamic contribution of textured thrust bearings during steady-state operation: a comparison with the untextured parallel surface configuration. Proc Inst Mech Eng Part J: J Eng Tribol 2014;229:362–75.

[38] Qiu Y, Khonsari MM. Experimental investigation of tribological performance of laser textured stainless steel rings. Tribol Int 2011;44:635–44.
[39] Bai LQ, Bai S. Frictional performance of a textured surface with elliptical dimples: geometric and distribution effects. Tribol Trans 2014;57:1122–8.
[40] Etsion I. Improving tribological performance of mechanical seals by laser surface texturing. Proceedings of the 17th international pump users symposium; 2000. p. 17.
[41] Yu XQ, He S, Cai RL. Frictional characteristics of mechanical seals with a laser-textured seal face. J Mater Process Technol 2002;129:463–6.
[42] Erdemir A. Review of engineered tribological interfaces for improved boundary lubrication. Tribol Int 2005;38:249–56.
[43] Wang L. Use of structured surfaces for friction and wear control on bearing surfaces. Surf Topogr: Metrol Prop 2014:2.
[44] Bruzzone AAG, Costa HL, Lonardo PM, Lucca DA. Advances in engineered surfaces for functional performance. CIRP Ann – Manuf Technol 2008;57:750–69.
[45] Sudeep U, Tandon N, Pandey RK. Performance of lubricated rolling/sliding concentrated contacts with surface textures: a review. J Tribol 2015;137:031501-1–031501-11.
[46] Yu H, Huang W, Wang X. Dimple patterns design for different circumstances. Lubr Sci 2013;25:67–78.
[47] Zhu D, Wang QJ. Elastohydrodynamic lubrication: a gateway to interfacial mechanics – review and prospect. J Tribol 2011;133:041001-.
[48] Coblas DG, Fatu A, Hajjam M. Manufacturing textured surfaces: state of art and recent developments. Proc Inst Mech Eng Part J: J Eng Tribol 2015;229:3–29.
[49] Venkatesan S. Surface textures for enhanced lubrication: fabrication and characterization techniques [University of Ketucky Master's thesis]. US: University of Ketucky; 2005.
[50] Costa HL, Hutchings IM. Some innovative surface texturing techniques for tribological purposes. Proc Mech Eng Part J – J Eng Tribol 2015;229:429–48.
[51] Stachowiak GW, Podsiadlo P. 3-D characterization, optimization, and classification of textured surfaces. Tribol Lett 2008;32:13–21.
[52] Wakuda M, Yamauchi Y, Kanzaki S, Yasuda Y. Effect of surface texturing on friction reduction between ceramic and steel materials under lubricated sliding contact. Wear 2003;254:356–63.
[53] Varenberg M, Halperin G, Etsion I. Different aspects of the role of wear debris in fretting wear. Wear 2002;252:902–10.
[54] Yamakiri H, Sasaki S, Kurita T, Kasashima N. Effects of laser surface texturing on friction behavior of silicon nitride under lubrication with water. Tribol Int 2011;44:579–84.
[55] Wan Y, Xiong D. The effect of laser surface texturing on frictional performance of face seal. J Mater Process Technol 2008;197:96–100.
[56] Kovalchenko A, Ajayi O, Erdemir A, Fenske G, Etsion I. The effect of laser surface texturing on transitions in lubrication regimes during unidirectional sliding contact. Tribol Int 2005;38:219–25.
[57] Ronen A, Etsion I, Kligerman Y. Friction-reducing surface-texturing in reciprocating automotive components. Tribol Trans 2001;44:359–66.
[58] Qiu Y, Khonsari MM. On the prediction of cavitation in dimples using a mass-conservative algorithm. J Tribol 2009;131:11.
[59] Zhang J, Meng Y. Direct observation of cavitation phenomenon and hydrodynamic lubrication analysis of textured surfaces. Tribol Lett 2012;46:147–58.
[60] Olver AV, Fowell MT, Spikes HA, Pegg IG. 'Inlet suction', a load support mechanism in non-convergent, pocketed, hydrodynamic bearings. Proc Inst Mech Eng Part J: J Eng Tribol 2006;220:105–8.
[61] Fowell MT, Olver AV, Gosman AD, Spikes HA, Pegg IG. Entrainment and inlet suction: two mechanisms of hydrodynamic lubrication in textured bearings. J Tribol 2007;129:336–47.
[62] Ausas RF, Ragot P, Leiva J, Jai M, Bayada G, Buscaglia GC. The impact of the cavitation model in the analysis of microtextured lubricated journal bearings. J Tribol 2007;129:868–75.
[63] Tønder K. Dynamics of rough slider bearings: effects of one-sided roughness/waviness. Tribol Int 1996;29:117–22.
[64] Tønder K. Hydrodynamic effects of tailored inlet roughnesses: extended theory. Tribol Int 2004;37:137–42.
[65] Arghir M, Roucou N, Helene M, Frene J. Theoretical analysis of the incompressible laminar flow in a macro-roughness cell. J Tribol 2003;125:309–18.
[66] Sahlin F, Glavatskih S, Tr Almqvist, Larsson R. Two-dimensional CFD-analysis of micro-patterned surfaces in hydrodynamic lubrication. J Tribol 2005;127:96–102.
[67] Dobrica MB, Fillon M. About the validity of Reynolds equation and inertia effects in textured sliders of infinite width. Proc Inst Mech Eng Part J: J Eng Tribol 2009;223:69–78.
[68] de Kraker A, van Ostayen RAJ, Rixen DJ. Development of a texture averaged Reynolds equation. Tribol Int 2010;43:2100–9.
[69] Cupillard S, Glavatskih S, Cervantes MJ. 3D thermohydrodynamic analysis of a textured slider. Tribol Int 2009;42:1487–95.
[70] Cupillard S, Cervantes MJ, Glavatskih S. Pressure buildup mechanism in a textured inlet of a hydrodynamic contact. J Tribol 2008;130:021701-.
[71] Cupillard S, Glavatskih S, Cervantes MJ. Inertia effects in textured hydrodynamic contacts. Proc Inst Mech Eng Part J: J Eng Tribol 2010;224:751–6.
[72] Cupillard S, Glavatskih S, Cervantes MJ. Computational fluid dynamics analysis of a journal bearing with surface texturing. J Eng Tribol 2008;222:97–108.
[73] Cupillard S, Cervantes MJ, Glavatskih SA. CFD study of a finite textured journal bearing. IAHR symposium on hydraulic machinery and systems. Foz do Iguassu, Brazil; 2008.
[74] Yagi K, Sugimura J. Balancing wedge action: a contribution of textured surface to hydrodynamic pressure generation. Tribol Lett 2013;50:349–64.
[75] Etsion I, Halperin G. A laser surface textured hydrostatic mechanical seal. Tribol Trans 2002;45:430–4.
[76] Kligerman Y, Etsion I, Shinkarenko A. Improving tribological performance of piston rings by partial surface texturing. J Tribol 2005;127:632–8.
[77] Ryk G, Kligerman Y, Etsion I, Shinkarenko A. Experimental investigation of partial laser surface texturing for piston-ring friction reduction. Tribol Trans 2005;48:583–8.
[78] Ryk G, Etsion I. Testing piston rings with partial laser surface texturing for friction reduction. Wear 2006;261:792–6.
[79] Bai S, Peng X, Li Y, Sheng S. A hydrodynamic laser surface-textured gas mechanical face seal. Tribol Lett 2010;38:187–94.
[80] Meng X, Bai S, Peng X. Lubrication film flow control by oriented dimples for liquid lubricated mechanical seals. Tribol Int 2014;77:132–41.
[81] Brunetiere N, Tournerie B. Numerical analysis of a surface-textured mechanical seal operating in mixed lubrication regime. Tribol Int 2012;49:80–9.
[82] Braun MJ, Hannon WM. Cavitation formation and modelling for fluid film bearings: a review. Proc Inst Mech Eng 2014;224:839–63.
[83] Qiu Y, Khonsari MM. Performance analysis of full-film textured surfaces with consideration of roughness effects. J Tribol 2011;133 (021704-1-10).
[84] Wang X, Kato K, Adachi K, Aizawa K. Loads carrying capacity map for the surface texture design of SiC thrust bearing sliding in water. Tribol Int 2003;36:189–97.
[85] Wang X, Adachi K, Otsuka K, Kato K. Optimization of the surface texture for silicon carbide sliding in water. Appl Surf Sci 2006;253:1282–6.
[86] Wang X, Wang J, Zhang B, Huang W. Design principles for the area density of dimple patterns. Proc Inst Mech Eng Part J – J Eng Tribol 2015;229:538–46.
[87] Rahmani R, Shirvani A, Shirvani H. Optimization of partially textured parallel thrust bearings with square-shaped micro-dimples. Tribol Trans 2007;50:401–6.
[88] Rahmani R, Mirzaee I, Shirvani A, Shirvani H. An analytical approach for analysis and optimisation of slider bearings with infinite width parallel textures. Tribol Int 2010;43:1551–65.
[89] Pascovici MD, Cicone T, Fillon M, Dobrica MB. Analytical investigation of a partially textured parallel slider. Proc Inst Mech Eng Part J: J Eng Tribol 2009;223:151–8.
[90] Guzek A, Podsiadlo P, Stachowiak GW. A unified computational approach to the optimization of surface textures:one dimensional hydrodynamic bearings. Tribol Online 2010;5:150–60.
[91] Guzek A, Podsiadlo P, Stachowiak GW. Optimization of textured surface in 2D parallel bearings governed by the Reynolds equation including cavitation and temperature. Tribol Online 2013;8:7–21.
[92] Gherca A, Fatu A, Hajjam M, Maspeyrot P. Effects of surface texturing in steady-state and transient flow conditions: Two-dimensional numerical simulation using a mass-conserving cavitation model. Proc Inst Mech Eng Part J: J Eng Tribol 2014;229:505–22.
[93] Malik S, Kakoty SK. Analysis of dimple textured parallel and inclined slider bearing. Proc Inst Mech Eng Part J: J Eng Tribol 2014;228:1343–57.
[94] Marian VG, Kilian M, Scholz W. Theoretical and experimental analysis of a partially textured thrust bearing with square dimples. Proc Inst Mech Eng Part J: J Eng Tribol 2007;221:771–8.
[95] Charitopoulos AG, Fouflias DG, Papadopoulos CI, Kaiktsis L, Fillon M. Thermohydrodynamic analysis of a textured sector-pad thrust bearing: effects on mechanical deformations. Mech Ind 2014;15:403–11.
[96] Fouflias DG, Charitopoulos AG, Papadopoulos CI, Kaiktsis L, Fillon M. Performance comparison between textured, pocket, and tapered-land sector-pad thrust bearings using computational fluid dynamics thermo-hydrodynamic analysis. Proc Inst Mech Eng Part J: J Eng Tribol 2014;229:376–97.
[97] Wang L, Wang W, Wang H, Ma T, Hu Y. Numerical analysis on the factors affecting the hydrodynamic performance for the parallel surfaces with microtextures. J Tribol 2014;136:021702-1–8.
[98] Cupillard S, Glavatskih S, Cervantes MJ. Thermal analysis of lubricant flow in a textured inlet contact. In: Kim JH, editor. Proceedings of the 19th international symposium on transport phenomena (ISTP-19). University of Iceland, Faculty of Industrial Engineering, Mechanical Engineering and Computer Science; 2008.
[99] Cameron A. Basic lubrication theory. 3rd ed.. London: Longman Group Ltd; 1971.
[100] Tønder K. Dimpled pivoted plane bearings: modified coefficients. Tribol Int 2010;43:2303–7.
[101] Tønder K. Micro- and macro-modifications of pivoted slider bearings: performance comparison and texturing versus width reduction. Tribol Int 2011;44:463–7.
[102] Patir N, Cheng HS. An average flow model for determining effects of three-dimensional roughness on partial hydrodynamic lubrication. J Tribol 1978;100:12–7.
[103] Papadopoulos CI, Efstathiou EE, Nikolakopoulos PG, Kaiktsis L. Geometry optimization of textured three-dimensional micro-thrust bearings. J Tribol 2011;133:041702-.

[104] Papadopoulos CI, Nikolakopoulos PG, Kaiktsis L. Characterization of stiffness and damping in textured sector pad micro thrust bearings using computational fluid dynamics. J Eng Gas Turbines Power 2012;134:112502-1–9.
[105] Brajdic-Mitidieri P, Gosman AD, Ioannides E, Spikes HA. CFD analysis of a low friction pocketed pad bearing. J Tribol 2005;127:803–12.
[106] Kango S, Sharma RK, Pandey RK. Comparative analysis of textured and grooved hydrodynamic journal bearing. Proc Inst Mech Eng Part J: J Eng Tribol 2014;228:82–95.
[107] Yu H, Wang X, Zhou F. Geometric shape effects of surface texture on the generation of hydrodynamic pressure between conformal contacting surfaces. Tribol Lett 2010;37:123–30.
[108] Etsion I. Modeling of surface texturing in hydrodynamic lubrication. Friction 2013;1:195–209.
[109] Yu H, Deng H, Huang W, Wang X. The effect of dimple shapes on friction of parallel surfaces. Proc Inst Mech Eng Part J: J Eng Tribol 2011;225:693–703.
[110] Qiu M, Delic A, Raeymaekers B. The effect of texture shape on the load-carrying capacity of gas-lubricated parallel slider bearings. Tribol Lett 2012;48:315–27.
[111] Qiu M, Minson BR, Raeymaekers B. The effect of texture shape on the friction coefficient and stiffness of gas-lubricated parallel slider bearings. Tribol Int 2013;67:278–88.
[112] Shen C, Khonsari MM. Numerical optimization of texture shape for parallel surfaces under unidirectional and bidirectional sliding. Tribol Int 2015;82:1–11.
[113] Nanbu T, Ren N, Yasuda Y, Zhu D, Wang QJ. Micro-textures in concentrated conformal-contact lubrication: effects of texture bottom shape and surface relative motion. Tribol Lett 2008;29:241–52.
[114] Shen C, Khonsari MM. Effect of Dimple's internal structure on hydrodynamic lubrication. Tribol Lett 2013;52:415–30.
[115] Qiu M, Raeymaekers B. The load-carrying capacity and friction coefficient of incompressible textured parallel slider bearings with surface roughness inside the texture features. Proc Inst Mech Eng Part J: J Eng Tribol 2014;229:547–56.
[116] Charitopoulos AG, Efstathiou EE, Papadopoulos CI, Nikolakopoulos PG, Kaiktsis L. Effects of manufacturing errors on tribological characteristics of 3-D textured micro- thrust bearings. CIRP J Manuf Sci Technol 2013;6:128–42.
[117] Reynolds O. On the theory of lubrication and its application to Mr. Beauchamp Tower's experiments, including an experimental determination of the viscosity of olive oil. Philos Trans R Soc Lond 1886;177:157–234.
[118] Caramia G, Carbone G, De Palma P. Hydrodynamic lubrication of micro-textured surfaces: two dimensional CFD-analysis. Tribol. Int 2015;88:162–9.
[119] Han J, Fang L, Sun J, Ge S. Hydrodynamic lubrication of microdimple textured surface using three-dimensional CFD. Tribol Trans 2010;53:860–70.
[120] Papadopoulos CI, Nikolakopoulos PG, Kaiktsis L. Evolutionary optimization of micro-thrust bearings with periodic partial trapezoidal surface texturing. J Eng Gas Turbines Power 2010;133:012301-.
[121] Feldman Y, Kligerman Y, Etsion I, Haber S. The validity of the Reynolds equation in modeling hydrostatic effects in gas lubricated textured parallel surfaces. J Tribol 2005;128:345–50.
[122] Qiu M, Bailey BN, Stoll R, Raeymaekers B. The accuracy of the compressible Reynolds equation for predicting the local pressure in gas-lubricated textured parallel slider bearings. Tribol Int 2014;72:83–9.
[123] Marian VG, Predescu A, Pascovici MD. Theoretical analysis of an infinitely wide rigid cylinder rotating over a grooved surface in hydrodynamic conditions. Proc Inst Mech Eng Part J: J Eng Tribol 2009;224:757–63.
[124] Jakobsson B, Floberg L. The finite journal bearing, considering vaporization. Goteborg, Sweden: Tran Chalmers University of Tech Gothenburg; 1957. p. 1–116.
[125] Olsson KO. Cavitation in dynamically loaded bearings. Goteborg, Sweden: Tran Chalmers University of Tech Gothenburg; 1965. p. 308.
[126] Elrod HG. A cavitation algorithm. J Tribol 1981;103:350–4.
[127] Elrod HG, Adams ML. A computer program for cavitation and starvation problems. Cavitation and related phenomena in lubrication. London, UK: Mechanical Engineering Publication; 1974. p. 37–41.
[128] Fesanghary M, Khonsari MM. A modification of the switch function in the elrod cavitation algorithm. J Tribol 2011;133:4.
[129] Brewe DE. Theoretical modeling of the vapor cavitation in dynamically loaded journal bearings. J Tribol 1986;108:628–37.
[130] Woods CM, Brewe DE. The solution of the Elrod algorithm for a dynamically loaded journal bearing using multigrid techniques. Tribology conference. Baltimore, Maryland; 1988.
[131] Vijayaraghavan D, Keith TG. Development and evaluation of a cavitation algorithm. Tribol Trans 1989;32:225–33.
[132] Vijayaraghavan D, Keith TG. An efficient, robust, and time accurate numerical scheme applied to a cavitation algorithm. J Tribol 1990;112:44–51.
[133] Kumar A, Booker JF. A finite element cavitation algorithm. J Tribol 1991;113:276–84.
[134] Kumar A, Booker JF. A finite element cavitation algorithm: application/validation. J Tribol 1991;113:255–60.
[135] Yi LY XIE, ShuangFu SUO, XiangFeng LIU, JingHao LI, YuMing WANG. A mass-conservative average flow model based on finite element method for complex textured surfaces. Sci China Phys Mech Astron 2013;56:1909–19.
[136] Shi F, Paranjpe R. An implicit finite element cavitation algorithm. Comput Model Eng Sci 2002;3:507–15.
[137] Hajjam M, Bonneau D. A transient finite element cavitation algorithm with application to radial lip seals. Tribol Int 2007;40:1258–69.
[138] Payvar P, Salant RF. A computational method for cavitation in a wavy mechanical seal. J Tribol 1992;114:199–204.
[139] Wang Y, Wang QJ, Lin C. Mixed lubrication of coupled journal-thrust-bearing systems including mass conserving cavitation. J Tribol 2003;125:747–55.
[140] Harp SR, Salant RF. An average flow model of rough surface lubrication with inter-asperity cavitation. J Tribol 2000;123:134–43.
[141] Shi F, Salant RF. A mixed soft elastohydrodynamic lubrication model with interasperity cavitation and surface shear deformation. J Tribol 1999;122:308–16.
[142] Xiong S, Wang QJ. Steady-state hydrodynamic lubrication modeled with the Payvar-Salant mass conservation model. J Tribol 2012;134:031703-.
[143] Sahlin F, Almqvist A, Larsson R, Glavatskih S. A cavitation algorithm for arbitrary lubricant compressibility. Tribol Int 2007;40:1294–300.
[144] Ausas RF, Jai M, Buscaglia GC. A mass-conserving algorithm for dynamical lubrication problems with cavitation. J Tribol 2009;131 (031702-1).
[145] Spencer A, Almqvist A, Larsson R. A semi-deterministic texture-roughness model of the piston ring–cylinder liner contact. Proc Inst Mech Eng Part J: J Eng Tribol 2011;225:325–33.
[146] Giacopini M, Fowell MT, Dini D, Strozzi A. A mass-conserving complementarity formulation to study lubricant films in the presence of cavitation. J Tribol 2010;132:041702-.
[147] Bertocchi L, Dini D, Giacopini M, Fowell MT, Baldini A. Fluid film lubrication in the presence of cavitation: a mass-conserving two-dimensional formulation for compressible, piezoviscous and non-Newtonian fluids. Tribol Int 2013;67:61–71.
[148] Medina S, Fowell MT, Vladescu S-C, Reddyhoff T, Pegg IG, Olver AV, et al. Transient effects in lubricated textured bearings. Proc Inst Mech Eng Part J: J Eng Tribol 2015;229:523–37.
[149] Woloszynski T, Podsiadlo P, Stachowiak GW. Efficient solution to the cavitation problem in hydrodynamic lubrication. Tribol Lett 2015;58:1–11.
[150] Hu Y, Zhu D. A full numerical solution to the mixed lubrication in point contacts. J Tribol 1999;122:1–9.
[151] Zhu D, Hu Y. A computer program package for the prediction of EHL and mixed lubrication characteristics, friction, subsurface stresses and flash temperatures based on measured 3-D surface roughness. Tribol Trans 2001;44:383–90.
[152] Epstein D, Keer LM, Wang QJ, Cheng HS, Zhu D. Effect of surface topography on contact fatigue in mixed lubrication. Tribol Trans 2003;46:506–13.
[153] Wang QJ, Zhu D. Virtual texturing: modeling the performance of lubricated contacts of engineered surfaces. J Tribol 2005;127:722–8.
[154] Wang QJ, Zhu D, Zhou R, Hashimoto F. Investigating the effect of surface finish on mixed EHL in rolling and rolling-sliding contacts. Tribol Trans 2008;51:748–61.
[155] Jiang X, Hua DY, Cheng HS, Ai X, Lee SC. A mixed elastohydrodynamic lubrication model with asperity contact. J Tribol 1999;121:481–91.
[156] Patir N, Cheng HS. Application of average flow model to lubrication between rough sliding surfaces. J Tribol 1979;101:220–9.
[157] Elrod HG. A general theory for laminar lubrication with Reynolds roughness. J Tribol 1979;101:8–14.
[158] Tripp JH. Surface roughness effects in hydrodynamic lubrication: the flow factor method. J Tribol 1983;105:458–63.
[159] Wu C, Zheng L. An average Reynolds equation for partial film lubrication with a contact factor. J Tribol 1989;111:188–91.
[160] Rocke AH, Salant RF. Elastohydrodynamic analysis of a rotary lip seal using flow factors. Tribol Trans 2005;48:308–16.
[161] Wilson WRD, Marsault N. Partial hydrodynamic lubrication with large fractional contact areas. J Tribol 1998;120:16–20.
[162] Chan C-W, Han Y-F, Wang Z, Wang J, Shi F, Wang N, et al. Exploration on a fast EHL computing technology for analyzing journal bearings with engineered surface textures. Tribol Trans 2013;57:206–15.
[163] de Kraker A, van Ostayen RAJ, van Beek A, Rixen DJ. A multiscale method modeling surface texture effects. J Tribol 2006;129:221–30.
[164] Dobrica MB, Fillon M, Maspeyrot P. Mixed elastohydrodynamic lubrication in a partial journal bearing – comparison between deterministic and stochastic models. J Tribol 2006;128:778–88.
[165] Elrod HG. Thin-film lubrication theory for newtonian fluids with surfaces possessing striated roughness or grooving. J Tribol 1973;95:484–9.
[166] Bayada G, Faure JB. A double scale analysis approach of the Reynolds roughness comments and application to the journal bearing. J Tribol 1989;111:323–30.
[167] Jai M, Bou-Saïd B. A comparison of homogenization and averaging techniques for the treatment of roughness in slip-flow-modified Reynolds equation. J Tribol 2001;124:327–35.
[168] Kane M, Bou-Said B. Comparison of homogenization and direct techniques for the treatment of roughness in incompressible lubrication. J Tribol 2004;126:733–7.
[169] Bayada G, Martin S, Vázquez C. An average flow model of the Reynolds roughness including a mass-flow preserving cavitation model. J Tribol 2005;127:793–802.
[170] Almqvist A, Dasht J. The homogenization process of the Reynolds equation describing compressible liquid flow. Tribol Int 2006;39:994–1002.
[171] Almqvist A, Essel EK, Persson LE, Wall P. Homogenization of the unstationary incompressible Reynolds equation. Tribol Int 2007;40:1344–50.
[172] Almqvist A, Lukkassen D, Meidell A, Wall P. New concepts of homogenization applied in rough surface hydrodynamic lubrication. Int J Eng Sci 2007;45:139–54.

[173] Sahlin F, Almqvist A, Larsson R, Glavatskih S. Rough surface flow factors in full film lubrication based on a homogenization technique. Tribol Int 2007;40:1025–34.
[174] Almqvist A, Essel EK, Fabricius J, Wall P. Reiterated homogenization applied in hydrodynamic lubrication. Proc Inst Mech Eng Part J: J Eng Tribol 2008;222:827–41.
[175] Sahlin F, Larsson R, Almqvist A, Lugt PM, Marklund P. A mixed lubrication model incorporating measured surface topography. Part 1: theory of flow factors. Proc Inst Mech Eng Part J: J Eng Tribol 2010;224:335–51.
[176] Sahlin F, Larsson R, Marklund P, Almqvist A, Lugt PM. A mixed lubrication model incorporating measured surface topography. Part 2: roughness treatment, model validation, and simulation. Proc Inst Mech Eng Part J: J Eng Tribol 2010;224:353–65.
[177] Almqvist A, Fabricius J, Spencer A, Wall P. Similarities and differences between the flow factor method by Patir and Cheng and homogenization. J Tribol 2011;133:031702-.
[178] Woloszynski T, Podsiadlo P, Stachowiak GW. Evaluation of discretisation and integration methods for the analysis of hydrodynamic bearings with and without surface texturing. Tribol Lett 2013;51:25–47.
[179] Woloszynski T, Podsiadlo P, Stachowiak GW. Evaluation of discretization and integration methods for the analysis of finite hydrodynamic bearings with surface texturing. Proc Inst Mech Eng Part J – J Eng Tribol 2015;229:465–77.
[180] Minet C, Brunetiere N, Tournerie B. A deterministic mixed lubrication model for mechanical seals. J Tribol 2011;133:042203-.
[181] Pei S, Ma S, Xu H, Wang F, Zhang Y. A multiscale method of modeling surface texture in hydrodynamic regime. Tribol Int 2011;44:1810–8.
[182] Arghir M, Alsayed A, Nicolas D. The finite volume solution of the Reynolds equation of lubrication with film discontinuities. Int J Mech Sci 2002;44:2119–32.
[183] Bonneau D, Fatu A, Souchet D. Hydrodynamic bearings. New York: ISTE, London and John Wiley & Sons; 2014.
[184] Dobrica MB, Fillon M. Reynolds' model suitability in simulating Rayleigh step bearing thermohydrodynamic problems. Tribol Trans 2005;48:522–30.
[185] Arghir M, Lez SL, Frene J. Finite-volume solution of the compressible Reynolds equation: linear and non-linear analysis of gas bearings. Proc Inst Mech Eng Part J: J Eng Tribol 2006;220:617–27.
[186] Buscaglia GC, Jai M. Homogenization of the generalized Reynolds equation for ultra-thin gas films and its resolution by FEM. J Tribol 2004;126:547–52.
[187] Sharma SC, Yadav SK. Performance analysis of a fully textured hybrid circular thrust pad bearing system operating with non-Newtonian lubricant. Tribol Int 2014;77:50–64.
[188] Almqvist A, Fabricius J, Larsson R, Wall P. A new approach for studying cavitation in lubrication. J Tribol 2013;136:011706-.
[189] Cottle RW, Pang JS, Stone RE. The linear complementarity problem: society for industrial and applied mathematics; 2009.
[190] Zhu D. On some aspects of numerical solutions of thin-film and mixed elastohydrodynamic lubrication. Proc Inst Mech Eng Part J: J Eng Tribol 2007;221:561–79.
[191] Wang W, Wang H, Liu Y, Hu Y, Zhu D. A comparative study of the methods for calculation of surface elastic deformation. Proc Inst Mech Eng Part J: J Eng Tribol 2003;217:145–54.
[192] Lugt PM, Morales-Espejel GE. A review of elasto-hydrodynamic lubrication theory. Tribol Trans 2011;54:470–96.
[193] Henry Y. Experimental analysis of the effect of pads texturing on fixed geometry hydrodynamic thrust bearings behavior [PhD thesis]. France: Université de Poitiers; 2013.